Game Theory and the COVID-19 Pandemic

INFORMS TutORials in Operations Research
https://doi.org/10.1287/educ.2021.0226

Anna Nagurney
Department of Operations and Information Management
Isenberg School of Management
University of Massachusetts
Amherst, Massachusetts 01003

Published October 2021

Abstract The world is now faced with the COVID-19 pandemic, a healthcare disaster, not limited to time or location. The COVID-19 pandemic has demonstrated the importance of operations research and related analytical tools, with the research and practitioner communities channeling and harnessing their expertise. It has inspired associated investigations and modeling and methodological advances in order to support deeper insights and enhanced decision-making as well as the provision of guidance to policy-makers. In this tutorial, I overview some of the novel advances and applications, inspired by the COVID-19 pandemic, utilizing game theory. The focus of the tutorial is on supply chain networks, although the scope is broader. The tutorial first presents an overview of variational inequality theory, which is the methodology utilized for the formulation, qualitative analysis, and solution of the described models. The supply chain network models presented are recently introduced ones that capture, respectively: the inclusion of labor into supply chain networks, enabling the quantitative assessment of disruptions to labor; the fierce competition among entities for medical supplies in the pandemic from PPEs to, now, vaccines; and, finally, the calculation of the potential synergy associated with the teaming, that is, the cooperation, among organizations in the pandemic, under cost and demand uncertainty, to provide needed supplies. Suggestions for future research are provided.

Keywords: COVID-19 pandemic, game theory, variational inequalities, supply chain networks, optimization

1. Introduction

On March 11, 2020, The World Health Organization declared the COVID-19 pandemic, due to the global spread of the novel coronavirus SARS-CoV-2, which causes the disease. The pandemic has impacted supply chains, commerce, and trade, employment and work, healthcare, transportation, education, entertainment, and social activities world-wide, affecting six continents. This pandemic is a disaster not limited in time and location - as is the case in many natural disasters - and has revealed major gaps in disaster preparedness and response. Economies and societies have undergone significant transformations in this pandemic, with effects that will linger and that we can expect will be long-studied. Raker, Zacher, and Lowe (2020) have noted that the pandemic is “a disaster of unprecedented scale and scope.” As of April 6, 2021, the global COVID-19 death toll surpassed 3 million, with the United States having the highest number of deaths in the world, at 555,000, accounting for about 19% of all deaths due to COVID-19 (cf. Abraham and Maan (2021)). By May 20, 2021, the World Health Organization statistics had reported around 3.4 million deaths globally due to COVID-19, with the official death toll very likely “significantly undercounted” (see Revill and Farge (2021)).

The COVID-19 pandemic has vividly demonstrated the importance of operations research and related analytical tools, with the research and practitioner communities channeling and harnessing their expertise. It has inspired associated investigations and modeling and methodological advances in order to support deeper insights and to enhance decision-making as well as the provision of guidance to policy-makers. Indeed, the COVID-19 pandemic, now officially over a year old, has given rise to a relevant scientific literature, which is growing. For example, Currie et al. (2020) identified many complex challenges due to the COVID-19 pandemic and discussed how simulation modelling can assist in supporting informed decision-making. Ivanov (2020) highlighted simulation-based research concentrating on the potential impacts on global supply chains of the COVID-19 pandemic. Queiroz et al. (2020), in turn, described a research agenda through a structured literature review of COVID-19 related work and supply chain research on earlier epidemics. Ivanov and Dolgui (2020) argued for the necessity of a new perspective due to the coronavirus COVID-19 outbreak through the use of what they termed: intertwined supply networks. Ivanov and Das (2020) proposed a global supply chain model with the inclusion of the ripple effect of an epidemic outbreak. The authors also discussed pandemic supply risk mitigation measures and possible recovery paths, along with prospective global supply chain (re)-designs. van Hoek (2020) explored empirically supply chain risks in the context of COVID-19, along with practice-based approaches to enhance supply chain resilience. Paul and Chowdhury (2020), in turn, presented a mathematical model that can handle both supply and demand disruptions and that can be solved analytically.

Choi (2021), in his panoramic paper, overviewed the operations research (OR) literature and practices related to pandemics (including COVID-19), to identify what challenges OR can assist in tackling under COVID-19. He classified the literature into three sets: “before pandemic,” “during pandemic,” and “after pandemic.” Choi’s presentation of the literature focused on three main parties: (1) governments, (2) healthcare and non-profit organizations, and (3) companies (i.e., business operations). Kaplan (2020), early on in the pandemic, constructed “scratch models,” which are mathematical models created from scratch in real time, due to the pressures from various stakeholders to assist in both understanding the COVID-19 pandemic and how best to respond, on a local level, in real-time, given the knowledge at the time. Applications that he considered in his paper included: recommending event crowd-size restrictions, surge planning for a hospital, timing decisions with respect to university activities, and scenario analyses to determine the impacts of alternative interventions, among others.

Interestingly, and, as noted in Nagurney (2020a), Craighead, Ketchen, and Darby (2020) discussed a spectrum of theories for addressing the impacts of the COVID-19 pandemic on supply chains, with an eye towards how different organizations responded, and how supply chains, along with the associated processes, can be re-tuned if and when another pandemic occurs. Game theory is among the theories that they highlighted.

1.1 Some Background on Game Theory and Relevant Literature

In this tutorial, I overview some of the novel advances and applications, inspired by the COVID-19 pandemic, utilizing game theory. The focus of the tutorial is on supply chain networks, although the scope is broader.

Game theory is a powerful formalism since it captures interactions among multiple decision-makers. As noted in Nagurney (2020a), scholars in disciplines from mathematics to business to even political science use game theory to understand how people (or even organizations and governments) are likely to make decisions in response to actions by others. Typically, in the game theory model setting, one identifies the "players" in the game, their strategies, reflected by variables that they control, along with their objective functions, usually represented as utility functions, that they seek to individually optimize, and that depend upon their strategies and the strategies of the other players. Furthermore, each of the players in the game has his/her strategies subject to constraints. There are noncooperative games, in which the players compete with one another as well as cooperative games. In a sense, game theory problems and models build upon classical optimization models, in which there is a single decision-maker seeking to determine an optimal solution, given an objective function, variables, and constraints.

Game theory is also a natural paradigm for quantitatively investigating many important issues arising from the COVID-19 pandemic. For example, numerous firms have been affected by various supply chain disruptions and, consequently, consumers have been as well. Examples of sectors that have suffered include food (meat packing plants, fresh produce harvesting, etc.) due to labor shortages, as a consequence of illnesses, deaths, decreases in productivity, as well as new measures of social distancing (cf. Polansek and Huffstutter (2020), Hardwick (2020), Corkery and

Yaffe-Bellany (2020), Corbishley (2020), Nagurney (2021b)). Technological product availability has also been adversely affected, due to, among other reasons, changes in consumer demand as workers increasingly work from home, with shortages of computer chips disrupting automobile manufacturing (see Whalen, Albergotti, and Lynch (2021)). Even blood supply chains have been disrupted in the pandemic (Nagurney (2020b)). The fierce competition among healthcare organizations as well as national governments, in turn, for Personal Protective Equipment (PPE) and other medical supplies, such as ventilators and testing kits, further illustrates the necessity of capturing the interactions among decision-makers in this new world scenario of the COVID-19 pandemic (cf. Burki (2020), Ranney, Griffeth, and Jha (2020), Nagurney et al. (2021)). More recently, there has been intense competition for vaccines among national governments and even on the individual level as supplies of vaccines remain limited and the demand for them immense (see Falcone (2020) and Walsh (2021)). Vaccines and mass vaccination are viewed as a gateway out of the pandemic and a return to lives closer to pre-pandemic "normality."

Hence, given that the COVID-19 pandemic is a disaster on a global scale and is also a healthcare disaster, it is important to highlight the relevant literature on game theory and disaster management. Historically, the literature on optimization and disaster management, especially with a focus on humanitarian logistics, has been growing in scope over the past two decades (cf. Balcik and Beamon (2008), Mete and Zabinsky (2010), Nagurney, Salarpour, and Daniele (2019) and the references therein). In such contexts it is essential to identify the appropriate objective functions and constraints with the former being distinct from, for example, profit maximization used widely in commercial supply chains (cf. Nagurney (2006) and the references therein). As an illustration, Tzeng, Cheng, and Huang (2007) constructed a dynamic selection of the volume of relief items to be transported from depots to demand points such that three objectives are achieved: minimum total cost, minimum travel time, and maximum demand satisfaction. Haghani and Oh (1996) in their classical paper considered commodity carry-over, routing, and mode transfer. Ozdamar, Ekinci, and Kkyazici (2004), Yi and Kumar (2007), and Yi and Ozdamar (2007) incorporated split delivery and the sum of unmet demands in their models. Vitoriano et al. (2011) proposed a multicriteria model for humanitarian relief distribution with criteria of time of response, equity, and security. Huang, Smilowitz, and Balcik (2012) captured several relevant disaster relief objectives of efficiency, efficacy, and equity with the consideration of both vehicle routing and resource distribution. For a variety of related issues and perspectives, we refer the reader to the volumes on Dynamics of Disasters edited by Kotsireas, Pardalos, and Nagurney (2018) and by Kotsireas et al. (2021).

With respect to game theory and disaster management, Muggy and Heier Stamm (2014) noted, in their survey on game theory and humanitarian operations, that applications had been limited. More recently, Seaberg, Devine, and Zhuang (2017) emphasized, in their review of 57 papers over the period 2006 to 2016, that the response phase of disaster management, which also includes the phases of mitigation, preparedness, and recovery, had been addressed most extensively. Subsequently, Coles, Zhang, and Zhuang (2018) noted the usefulness of noncooperative game theory in aiding different agencies and organizations, as well as governments, plus NGOs, in enhanced decision-making, along with the identification of partnerships during response and recovery phases. Earlier, Coles and Zhuang (2011) had discussed the relevance of cooperative game theory in disaster recovery operations. Nagurney and Qiang (2020), in turn, identified potential synergies in the teaming of humanitarian organizations in disaster relief, using a supply chain network paradigm. Mamani, Chick, and Simchi-Levi (2013) in their game theory paper, also of relevance to the COVID-19 pandemic, demonstrated that lack of coordination can lead to unbalanced distribution and shortages (or excesses) of influenza vaccines. Cost-sharing contracts could, in turn, enhance global vaccine allocation, through increased coordination.

Of particular relevance in the COVID-19 pandemic are Generalized Nash Equilibrium (GNE) models (cf. Debreu (1952), Rosen (1965)), in which not only do the utility functions of the players in the game depend on each others' strategies, but their respective feasible sets do, as well. In Nash Equilibrium problems (see Nash (1950, 1951)) of well-known noncooperative games, only the utility functions depend on the strategies of the players and the feasible sets do not. Pre-pandemic, the first GNE model for disaster relief was constructed by Nagurney, Alvarez Flores, and Soylu (2016), who integrated both logistical and financial aspects of humanitarian organizations (see also Toyasaki and Wakolbinger (2014)), and, because of the underlying objective functions, were able to construct an optimization formulation. Subsequently, Nagurney, Salarpour, and Daniele (2019) used the concept of a Variational Equilibrium (cf. Kulkarni and Shanbhag (2012)) to construct a variational inequality formulation of an integrated financial and logistical model for disaster relief, under budget constraints. Additional relevant research on game theory and disaster management can be found in the papers of Nagurney et al. (2018), Gossler et al. (2019), and Nagurney et al. (2020), where the first stochastic Generalized Nash Equilibrium model for disaster relief was constructed, in which each relief organization is faced with a two-stage stochastic optimization problem (see also Rawls and Turnquist (2010), Salmeron and Apte (2010), Mete and Zabinsky (2010), Falasca and Zobel (2011), Grass and Fischer (2016)).

1.2 Organization of this Tutorial

In Section 2, we overview some of the fundamentals of variational inequality theory in order to document the methodological tools in the formulation, analysis, and solution of various game theory models inspired by the COVID-19 pandemic. In Sections 3, 4, and 5 we present various applications. Specifically, in Section 3, we focus on the commercial sector and present a game theory model of supply chain network competition in which labor is a critical resource. The governing equilibrium concept therein is that of a Nash equilibrium. In Section 4, we then discuss a Generalized Nash Equilibrium model focusing on competition for medical supplies under demand uncertainty. Section 5 then turns to the study of cooperation among organizations and highlights a measure to quantify synergy in the case of multiproduct supply chains, using a mean-variance approach. Additional relevant literature is highlighted within each of these sections. Section 6 concludes this tutorial and also highlights directions for future research.

2. Methodology

In this section, some of the fundamental theory is recalled, beginning with variational inequality theory and segueing to game theory and its relationship to the former. The various proofs can be found in Nagurney (1999) and in the classical book by Kinderlehrer and Stampacchia (1980), with additional references noted, as appropriate.

2.1 Variational Inequality Theory

In this subsection, a brief overview of the theory of variational inequalities is given, including qualitative results, notably, regarding the existence and uniqueness of solutions. All definitions and theorems are taken from Nagurney (1999). All vectors are assumed to be column vectors.

Definition 2.1: Finite-Dimensional Variational Inequality Problem

The finite-dimensional variational inequality problem, $\mathrm{VI}(F, \mathcal{K})$*, is to determine a vector* $X^* \in \mathcal{K} \subset R^N$*, such that*

$$\langle F(X^*), X - X^* \rangle \geq 0, \quad \forall X \in \mathcal{K}, \tag{2.1a}$$

where F *is a given continuous function from* $\mathcal{K}$ *to* R^N*,* $\mathcal{K}$ *is a given closed convex set, and* $\langle \cdot, \cdot \rangle$ *denotes the inner product in* N*-dimensional Euclidean space. In (2.1a),* $F(X) \equiv (F_1(X), F_2(X), \ldots, F_N(X))^T$*, and* $X \equiv (X_1, X_2, \ldots, X_N)^T$*. Recall that for two vectors* $u, v \in \mathcal{R}^N$*, the inner product* $\langle u, v \rangle = \|u\| \|v\| cos\theta$*, where* θ *is the angle between the vectors* u *and* v*, and (2.1a) is equivalent to*

$$\sum_{i=1}^{N} F_i(X^*) \cdot (X_i - X_i^*) \geq 0, \quad \forall X \in \mathcal{K}. \tag{2.1b}$$

The variational inequality problem is a general problem construct that encompasses a wide spectrum of mathematical programming problems, including: optimization problems, complementarity problems, and is also related to fixed point problems (see Nagurney (1999)). It has been shown that optimization problems, both constrained and unconstrained, can be reformulated as variational inequality problems. The relationship between variational inequalities and optimization problems is now reviewed.

Proposition 2.1: Formulation of a Constrained Optimization Problem as a Variational Inequality

Let X^* be a solution to the optimization problem:

$$Minimize \quad f(X) \tag{2.2}$$

subject to:

$$X \in \mathcal{K},$$

where f is continuously differentiable and $\mathcal{K}$ is closed and convex. Then X^* is a solution of the variational inequality problem:

$$\langle \nabla f(X^*), X - X^* \rangle \geq 0, \quad \forall X \in \mathcal{K}, \tag{2.3}$$

where $\nabla f(X)$ is the gradient vector of f with respect to X; that is, $\nabla f(X) \equiv (\frac{\partial f(X)}{\partial X_1}, \ldots, \frac{\partial f(X)}{\partial X_N})^T$.

Proposition 2.2: Formulation of an Unconstrained Optimization Problem as a Variational Inequality

If $f(X)$ is a convex function and X^* is a solution to $\mathrm{VI}(\nabla f, \mathcal{K})$*, then X^* is a solution to the optimization problem (2.2). In the case that the feasible set $\mathcal{K} = R^N$, then the unconstrained optimization problem is also a variational inequality problem.*

The variational inequality problem can be reformulated as an optimization problem under certain symmetry conditions. Several definitions are now recalled, followed by a theorem presenting the above relationship.

Definition 2.2: Positive Semi-Definiteness and Definiteness

An $N \times N$ matrix $M(X)$, whose elements $m_{ij}(X); i, j = 1, ..., N$, are functions defined on the set $\mathcal{T} \subset R^N$, is said to be positive-semidefinite on $\mathcal{T}$ if

$$v^T M(X) v \geq 0, \quad \forall v \in R^N, \, X \in \mathcal{T}. \tag{2.4}$$

It is said to be positive-definite on $\mathcal{T}$ if

$$v^T M(X) v > 0, \quad \forall v \neq 0, \, v \in R^N, \, X \in \mathcal{T}. \tag{2.5}$$

Finally, it is said to be strongly positive-definite on $\mathcal{T}$ if

$$v^T M(X) v \geq \alpha \|v\|^2, \textit{ for some } \alpha > 0, \quad \forall v \in R^N,\ X \in \mathcal{T}. \tag{2.6}$$

Theorem 2.1: Reformulation of a Variational Inequality Problem as an Optimization Problem Under Symmetry Assumption

Assume that $F(X)$ is continuously differentiable on $\mathcal{K}$ and that the Jacobian matrix

$$\nabla F(X) = \begin{bmatrix} \frac{\partial F_1}{\partial X_1} & \cdots & \frac{\partial F_1}{\partial X_N} \\ \vdots & \cdots & \vdots \\ \frac{\partial F_N}{\partial X_1} & \cdots & \frac{\partial F_N}{\partial X_N} \end{bmatrix} \tag{2.7}$$

is symmetric and positive-semidefinite. Then there is a real-valued convex function $f : \mathcal{K} \longmapsto R^1$ satisfying

$$\nabla f(X) = F(X) \tag{2.8}$$

with X^* the solution of VI$(F, \mathcal{K})$ *also being the solution of the mathematical programming problem:*

$$\textit{Minimize} \quad f(X)$$

subject to:

$$X \in \mathcal{K},$$

where $f(X) = \int F(X)^T dx$, and $\int$ is a line integral.

Hence, the variational inequality is a more general problem formulation than an optimization problem formulation, since it can also handle a function $F(X)$ with an asymmetric Jacobian (see Nagurney (1999)). This enriches the breadth of applications that can be rigorously handled in different disciplines. Next, certain qualitative properties associated with variational inequality problems are presented.

Existence of a solution to a variational inequality problem follows from continuity of the function $F(X)$ that enters the variational inequality, provided that the feasible set $\mathcal{K}$ is compact as stated in Theorem 2.2.

Theorem 2.2: Existence of a Solution

If $\mathcal{K}$ is a compact convex set and $F(X)$ is continuous on $\mathcal{K}$, then the variational inequality problem admits at least one solution X^*.

Theorem 2.3: Existence of a Solution Using a Coercivity Condition

Suppose that $F(X)$ satisfies the coercivity condition

$$\frac{\langle F(X) - F(X_0), X - X_0 \rangle}{\|X - X_0\|} \to \infty \tag{2.9}$$

as $\|X\| \to \infty$ for $X \in \mathcal{K}$ and for some $X_0 \in \mathcal{K}$. Then $\mathrm{VI}(F, \mathcal{K})$ always has a solution.

According to the above theorem, existence of a solution to a variational inequality problem is guaranteed if the coercivity condition holds. Below, various monotonicity conditions are utilized in addressing the qualitative properties of existence and uniqueness of solutions, but, first, basic definitions of monotonicity are provided.

Definition 2.3: Monotonicity

$F(X)$ is monotone on $\mathcal{K}$ if

$$\langle F(X^1) - F(X^2), X^1 - X^2 \rangle \geq 0, \quad \forall X^1, X^2 \in \mathcal{K}. \tag{2.10}$$

Definition 2.4: Strict Monotonicity

$F(X)$ is strictly monotone on $\mathcal{K}$ if

$$\langle F(X^1) - F(X^2), X^1 - X^2 \rangle > 0, \quad \forall X^1, X^2 \in \mathcal{K},\ X^1 \neq X^2. \tag{2.11}$$

Definition 2.5: Strong Monotonicity

$F(X)$ is strongly monotone on $\mathcal{K}$ if

$$\langle F(X^1) - F(X^2), X^1 - X^2 \rangle \geq \alpha \|X^1 - X^2\|^2, \quad \forall X^1, X^2 \in \mathcal{K}, \tag{2.12}$$

where $\alpha > 0$.

Definition 2.6: Lipschitz Continuity

$F(X)$ is Lipschitz continuous on $\mathcal{K}$ if there exists an $L > 0$, such that

$$\langle F(X^1) - F(X^2), X^1 - X^2 \rangle \leq L \|X^1 - X^2\|^2, \quad \forall X^1, X^2 \in \mathcal{K}, \tag{2.13}$$

where L is known as the Lipschitz constant.

Theorem 2.4: Uniqueness of a Solution Under Strict Monotonicity

Suppose that $F(X)$ is strictly monotone on $\mathcal{K}$. Then the solution to the $\mathrm{VI}(F, \mathcal{K})$ *problem is unique, if one exists.*

Theorem 2.5: Existence and Uniqueness Under Strong Monotonicity

Suppose that $F(X)$ is strongly monotone on $\mathcal{K}$. Then there exists precisely one solution X^* to $\mathrm{VI}(F, \mathcal{K})$.

Note that, according to Theorem 2.5, strong monotonicity of the function F guarantees both existence and uniqueness of a solution, in the case of an unbounded feasible set $\mathcal{K}$. If the feasible set $\mathcal{K}$ is compact, that is, closed and bounded, the continuity of F guarantees the existence of a solution. The strict monotonicity of F is then sufficient to guarantee the uniqueness of a solution, provided that it exists.

2.2 The Relationships between Variational Inequalities and Game Theory

In this section, some of the relationships between variational inequalities and game theory are briefly discussed.

Nash (1950, 1951) developed noncooperative game theory, involving multiple players, each of whom acts in his/her own interest. In particular, consider a game with m players, each player i having, without loss of generality, a strategy vector $X_i = \{X_{i1}, ..., X_{in}\}$ selected from a closed, convex set $K_i \subset R^n$. Each player i seeks to maximize his/her own utility function, $U_i\colon \mathcal{K} \to \mathcal{R}$, where $\mathcal{K} = K_1 \times K_2 \times \cdots \times K_m \subset R^{mn}$. The utility of player i, U_i, depends not only on his/her own strategy vector, X_i, but also on the strategy vectors of all the other players, $(X_1, \ldots, X_{i-1}, X_{i+1}, \ldots, X_m)$. An equilibrium is achieved if no one can increase his/her utility by unilaterally altering the value of its strategy vector. The formal definition of the Nash equilibrium is as follows.

Definition 2.7: Nash Equilibrium

A Nash equilibrium is a strategy vector

$$X^* = (X_1^*, \ldots, X_m^*) \in \mathcal{K}, \tag{2.14}$$

where

$$U_i(X_i^*, \hat{X}_i^*) \geq U_i(X_i, \hat{X}_i^*), \quad \forall X_i \in K_i, \forall i, \tag{2.15}$$

and $\hat{X}_i^* = (X_1^*, \ldots, X_{i-1}^*, X_{i+1}^*, \ldots, X_m^*)$.

It has been shown by Hartman and Stampacchia (1966) and Gabay and Moulin (1980) that, given continuously differentiable and concave utility functions, U_i, $\forall i$, the Nash equilibrium problem can be formulated as a variational inequality problem defined on $\mathcal{K}$.

Theorem 2.6: Variational Inequality Formulation of Nash Equilibrium

Under the assumption that each utility function U_i is continuously differentiable and concave, X^* is a Nash equilibrium if and only if $X^* \in \mathcal{K}$ is a solution of the variational inequality

$$\langle F(X^*), X - X^* \rangle \geq 0, \quad X \in \mathcal{K}, \tag{2.16}$$

where $F(X) \equiv (-\nabla_{X_1} U_1(X), \ldots, -\nabla_{X_m} U_m(X))^T$, and $\nabla_{X_i} U_i(X) = (\frac{\partial U_i(X)}{\partial X_{i1}}, \ldots, \frac{\partial U_i(X)}{\partial X_{in}})$.

The conditions for existence and uniqueness of a Nash equilibrium are now introduced. As stated in the following theorem, Rosen (1965) presented existence under the assumptions that $\mathcal{K}$ is compact and each U_i is continuously differentiable.

Theorem 2.7: Existence of a Solution Under Compactness and Continuity

Suppose that the feasible set $\mathcal{K}$ is compact and that each U_i is continuously differentiable $\forall i$. Then existence of a Nash equilibrium is guaranteed.

Gabay and Moulin (1980) relaxed the assumption of compactness of $\mathcal{K}$ and established existence of a Nash equilibrium after imposing a coercivity condition on $F(X)$.

Theorem 2.8: Existence of a Solution Under Coercivity

Suppose that $F(X)$, as given in Theorem 2.6, satisfies the coercivity condition (2.9). Then there exists a Nash equilibrium.

Karamardian (1969), earlier, established existence and uniqueness of a Nash equilibrium under the strong monotonicity assumption.

Theorem 2.9: Existence and Uniqueness of a Solution Under Strong Monotonicity

Assume that $F(X)$, as given in Theorem 2.6, is strongly monotone on $\mathcal{K}$. Then there exists precisely one Nash equilibrium X^*.

Additionally, based on Theorem 2.4, uniqueness of a Nash equilibrium can be guaranteed under the assumptions that $F(X)$ is strictly monotone and that an equilibrium exists.

Theorem 2.10: Uniqueness of a Solution Under Strict Monotonicity

Suppose that $F(X)$, as given in Theorem 2.6, is strictly monotone on $\mathcal{K}$. Then the Nash equilibrium,

X^*, is unique, if it exists.

It is important to note that one can construct associated dynamic adjustment or tatonnenment processes associated with the players in a game. For background material on the theory of projected dynamical systems, see Dupuis and Nagurney (1993) and Nagurney and Zhang (1996), where additional results can be found, including conditions under which the set of stationary points of a projected dynamical system, which is a nonclassical dynamic system, coincides with the set of solutions to the related variational inequality problem. In the latter reference, stability analysis results are presented, of relevance to game theory problems as well as to a variety of equilibrium problems that have been formulated as variational inequality problems, from traffic network equilibrium problems to spatial price equilibrium problems and even financial network problems.

We now turn to a discussion of Generalized Nash Equilibrium (GNE) in which the constraints underlying the players' strategies also depend on the strategies of their rivals. A frequently encountered class of Generalized Nash games considers common coupling constraints that the players' strategies are required to satisfy (Kulkarni and Shanbhag (2012)). These games are also known as Generalized Nash games with shared constraints (Rosen (1965), Facchinei and Kanow (2007), Fischer, Herrich, and Schonefeld (2014)).

Definition 2.10: Generalized Nash Equilibrium

A strategy vector $X^* \in K \equiv \prod_{i=1}^m K_i, X^* \in \mathcal{S}$, constitutes a Generalized Nash Equilibrium if for each player i; $i = 1, ..., m$:

$$U_i(X_i^*, \hat{X}_i^*) \geq U_i(X_i, \hat{X}_i^*), \quad \forall X_i \in K_i, \forall X \in \mathcal{S}, \tag{2.17}$$

where

$$\hat{X}_i^* \equiv (X_1^*, \ldots, X_{i-1}^*, X_{i+1}^*, \ldots, X_m^*),$$

K_i is the feasible set of individual player i and $\mathcal{S}$ is the feasible set consisting of the shared constraints.

Bensoussan (1974) formulated the GNE problem as a quasivariational inequality. Nevertheless, it is recognized that GNE problems are challenging to solve as quasivariational inequality problems since the state-of-the-art in terms of algorithmics is not as advanced as that for variational inequality problems. Kulkarni and Shanbhag (2012) provide sufficient conditions to establish the theory of a *Variational Equilibrium* as a refinement of the GNE, which is highly relevant to applications in the COVID-19 pandemic, which we present later in this tutorial.

Definition 2.11: Variational Equilibrium

A strategy vector X^* is said to be a variational equilibrium of the above Generalized Nash Equilib-

rium game if $X^* \in \mathcal{K}$, where $\mathcal{K} \equiv K \cap \mathcal{S}$, is a solution of the variational inequality:

$$-\sum_{i=1}^{m} \langle \nabla_{X_i} \hat{U}_i(X^*), X_i - X_i^* \rangle \geq 0, \quad \forall X \in \mathcal{K}. \tag{2.18}$$

2.3 An Algorithm

There are many algorithms for the computation of solutions to variational inequality problems, including those based on the general iterative schemes of Dafermos (1983) and Dupuis and Nagurney (1993). In this tutorial, we use the modified projection method of Korpelevich (1977), which requires only Lipschitz continuity and monotonicity of $F(X)$ for convergence, provided a solution exists. We especially are interested in algorithms that resolve the variational inequality problem into subproblems that can be solved easily and exactly in closed form.

The modified projection method, with τ denoting an iteration counter, is presented below.

Step 0: Initialization

Set $X^0 \in \mathcal{K}$. Let $\tau = 1$ and let β be a scalar such that $0 < \beta \leq \frac{1}{L}$, where L is the Lipschitz continuity constant (cf. (2.13)).

Step 1: Computation

Compute $\bar{X}^\tau$ by solving the variational inequality subproblem:

$$\langle \bar{X}^\tau + \beta F(X^{\tau-1}) - X^{\tau-1}, X - \bar{X}^\tau \rangle \geq 0, \quad \forall X \in \mathcal{K}. \tag{2.19}$$

Step 2: Adaptation

Compute X^τ by solving the variational inequality subproblem:

$$\langle X^\tau + \beta F(\bar{X}^\tau) - X^{\tau-1}, X - X^\tau \rangle \geq 0, \quad \forall X \in \mathcal{K}. \tag{2.20}$$

Step 3: Convergence Verification

If $\max |X_l^\tau - X_l^{\tau-1}| \leq \epsilon$, for all l, with $\epsilon > 0$, a prespecified tolerance, then stop; else, set $\tau := \tau + 1$, and go to Step 1.

Theorem 2.11: Convergence of the Modified Projection Method

If $F(X)$ is monotone and Lipschitz continuous (and a solution exists), the modified projection algorithm converges to a solution of variational inequality (2.1a).

We now present several important models and applications relevant to the COVID-19 pandemic and beyond.

3. Commercial Supply Chains and the Inclusion of Labor

The COVID-19 pandemic has vividly and dramatically impacted labor, with workers getting ill, some perishing, whereas others have experienced decreases in productivity. Some workers have not been able to travel to locations where fresh produce needed to be picked, whereas others, including seafarers were "stuck" on ships, due to visa issues and fears of the coronavirus, affecting trade, as well as their well-being. Although economists have long considered labor as a critical resource, along with capital, in various production functions, the inclusion of labor into general supply chains, with an OR framework, did not occur until the pandemic struck.

Nagurney (2021b) constructed the first supply chain network optimization model that included labor and labor productivity factors associated with each link in the supply chain subject to a capacity on each link of labor, reflecting availability. That paper focused on perishable food products, since the food sector was one of the sectors greatly affected in a negative manner by labor shortages in the pandemic with food workers, including pickers, processors, etc., being recognized as essential workers (see IHS Markit (2020), Knight (2020)). That model used concepts of generalized networks from Yu and Nagurney (2013); see also Besik and Nagurney (2017) and Nagurney et al. (2017), to capture perishability of the food products as they move on pathways from origin nodes to destination nodes. Nagurney (2021c), focusing on supply chain networks where perishability of products is not a factor, proposed other sets of constraints on labor. In addition to capacities of labor on links, she considered capacities of labor availability associated with different supply chain network economic activities, such as production/manufacturing, storage/distribution, as well as transportation, followed by a single bound on labor availability in the supply chain network, with labor able to move across supply chain network economic activities. All the above models were formulated, analyzed, and numerical examples solved, using the theory of variational inequalities, with an eye towards the construction of game theoretic extensions.

Nagurney (2021a) proposed the first game theory framework for the inclusion of labor in competitive supply chain networks under three sets of constraints. The first model, which we highlight in this section, was a Nash Equilibrium one, since the bounds on labor were associated with the individual links of the various competing firms. In contrast, with bounds on labor associated with production, and, correspondingly, with storage, and with transportation, the firms' strategies were also constrained by these common, that is, shared constraints. Hence, the formalism therein, and also for the final case of a capacitated labor amount in the supply chain network economy that all the firms competed for and with labor free to move from activity to activity, was that of a Generalized Nash Equilibrium.

3.1 The Supply Chain Network Game Theory Model with Labor Bounds on Links

This model, and extensions, are due Nagurney (2021a), where additional results can be found. Here we adapt the notation therein to conform more closely to that in Section 2. We consider m firms that are involved in the production of a substitutable product and compete noncooperatively in the various supply chain network economic activities of: production, transportation, storage, and distribution of their products to consumers at the demand markets. The firms also compete with one another for labor, since labor is essential to the above network economic activities. Each firm is represented as a network of its economic activities as drawn in Figure 1. Note that the supply chain networks of the individual firms do not have any links in common. The notation for the model is given in Table 1.

Each firm i; $i = 1, \ldots, m$, owns n^i_M production facilities; has available n^i_D distribution centers, and serves n_R demand markets. Let L^i denote the links comprising the supply chain network of firm i; $i = 1, \ldots, m$, that it owns/controls, with a total of n_{L^i} elements. The links of L^i include firm i's links to its production nodes; the links from production nodes to the distribution centers, the storage links, and the links from the distribution centers to the demand markets. L then denotes the full set of links in the supply chain network economy with $L = \cup_{i=1}^m L^i$ containing a total of n_L elements. Let now $G = [\mathcal{N}, L]$ denote the graph consisting of the set of nodes $\mathcal{N}$ and the set of links L in Figure 1. Each firm seeks to determine its optimal product quantities that maximize its profits.

Observe that production links from the top-tiered nodes i; $i = 1, \ldots, m$, representing firm i, in the figure are joined to the production nodes of firm i, which are denoted, respectively, by: $M^i_1, \ldots, M^i_{n^i_M}$. The links from the production nodes, are then connected to the distribution center nodes of each firm i; $i = 1, \ldots, m$, and correspond to transportation links. These nodes are denoted by $D^i_{1,1}, \ldots, D^i_{n^i_D,1}$. The links joining nodes $D^i_{1,1}, \ldots, D^i_{n^i_D,1}$ with nodes $D^i_{1,2}, \ldots, D^i_{n^i_D,2}$ are the storage links. There are also distribution links joining the nodes $D^i_{1,2}, \ldots, D^i_{n^i_D,2}$ for $i = 1, \ldots, m$, with the bottom demand market nodes: $1, \ldots, n_R$. We also consider links connecting the production nodes with the demand market nodes to represent direct shipments to the demand markets, of high relevance in the pandemic, as in the case of electronic commerce. Of course, such links can also denote direct deliveries to consumers in the case that the producers are farms. Note that such distribution channels have been observed in the pandemic, as well (see, for example, Shea (2020)).

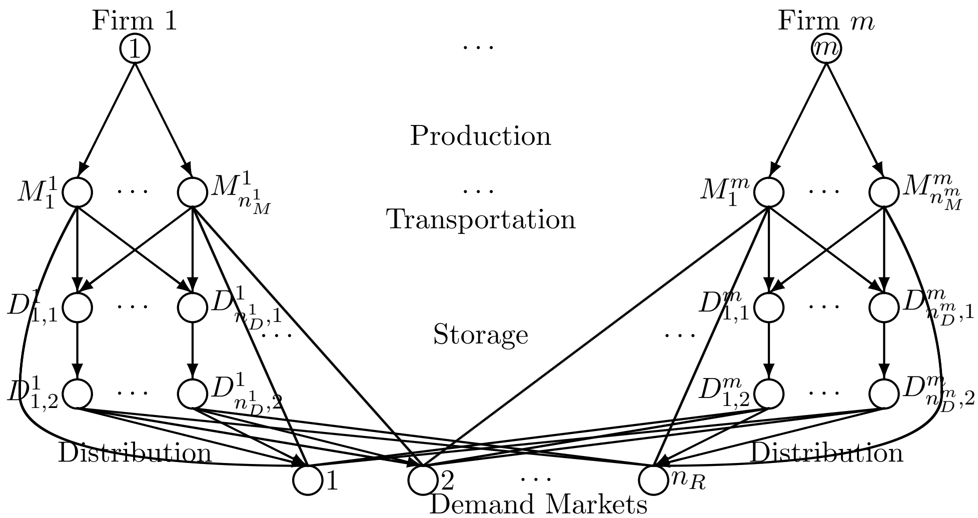

Figure 1: The Supply Chain Network Topology of the Game Theory Model with Labor

Table 1: Notation for the Supply Chain Game Theory Modeling Framework with Labor

Notation	**Definition**
P_k^i	the set of paths in firm i's supply chain network terminating in demand market k; $i = 1, \ldots, m$; $k = 1, \ldots, n_R$.
P^i	the set of all n_{P^i} paths of firm i; $i = 1, \ldots, m$.
P	the set of all n_P paths in the supply chain network economy.
$x_p; p \in P_k^i$	the nonnegative flow on path p originating at firm node i and terminating at demand market k; $i = 1, \ldots, m$; $k = 1, \ldots, n_R$. We group firm i's product path flows into the vector $x^i \in R_+^{n_{P^i}}$. We emphasize that x^i is the vector of strategic variables of firm i. We then group all the firms' product path flows into the vector $x \in R_+^{n_P}$.
f_a	the nonnegative flow of the product on link a, $\forall a \in L$. We group all the link flows into the vector $f \in R_+^{n_L}$.
l_a	the labor on link a (usually denoted in person hours).
α_a	positive factor relating input of labor to output of product flow on link a, $\forall a \in L$.
$\bar{l}_a$	the upper bound on the availability of labor on link a, $\forall a \in L$.
d_{ik}	the demand for the product of firm i at demand market k; $i = 1, \ldots, m$; $k = 1, \ldots, n_R$. We group the $\{d_{ik}\}$ elements for firm i into the vector $d^i \in R_+^{n_R}$ and all the demands into the vector $d \in R_+^{m \times n_R}$.
$\hat{c}_a(f)$	the total operational cost associated with link a, $\forall a \in L$.
π_a	cost of a unit of labor on link a.
$\rho_{ik}(d)$	the demand price function for the product of firm i at demand market k; $i = 1, \ldots, m$; $k = 1, \ldots, n_R$.

We emphasize that the topology of the supply chain networks for all the firms in Figure 1 can be modified/adapted accordingly to reflect a specific product and application under consideration.

The conservation of flow equations, guaranteeing that the demand for each firm's product is satisfied by the product shipments, is as follows, for each firm i: $i = 1, \ldots, m$:

$$\sum_{p \in P_k^i} x_p = d_{ik}, \quad k = 1, \ldots, n_R. \tag{3.1}$$

The path flows must be nonnegative; that is, for each firm i; $i = 1, \ldots, m$:

$$x_p \geq 0, \quad \forall p \in P^i. \tag{3.2}$$

The link flows of each firm i; $i = 1, \ldots, m$, in turn, are related to the path flows by the expression:

$$f_a = \sum_{p \in P} x_p \delta_{ap}, \quad \forall a \in L^i, \tag{3.3}$$

where $\delta_{ap} = 1$, if link a is contained in path p, and 0, otherwise. (3.3) states that the product flow of a firm on a link is equal to the sum of that product's flows on paths that contain that link.

As in Nagurney (2021a,b,c), we assume here that the product output on each link is a linear function of the labor input. This corresponds to a linear production function in economics (cf. Mishra (2007)). Thus, we have that

$$f_a = \alpha_a l_a, \quad \forall a \in L^i, \quad i = 1, \ldots, m. \tag{3.4}$$

Observe that the greater the value of α_a, the more productive labor is on the link.

The utility function of firm i, U_i; $i = 1, \ldots, m$, denotes the profit, which is given by the difference between its revenue and its total costs:

$$U_i = \sum_{k=1}^{n_R} \rho_{ik}(d) d_{ik} - \sum_{a \in L^i} \hat{c}_a(f) - \sum_{a \in L^i} \pi_a l_a. \tag{3.5a}$$

The first expression after the equal sign in (3.5a) is the revenue of firm i. The second one in (3.5) is the total operational costs for the supply chain network L^i of firm i, whereas the third expression is the total labor costs of firm i. The functions U_i; $i = 1, \ldots, m$, are assumed to be concave, with the demand price functions being monotone decreasing and continuously differentiable and the total link cost functions being convex and also continuously differentiable.

The optimization problem of each firm i; $i = 1, \ldots, m$, is, hence, given by:

$$\text{Maximize} \quad \sum_{k=1}^{n_R} \rho_{ik}(d) d_{ik} - \sum_{a \in L^i} \hat{c}_a(f) - \sum_{a \in L^i} \pi_a l_a, \tag{3.5b}$$

subject to: (3.1), (3.2), (3.3), and (3.4).

The additional constraints on the fundamental supply chain network model described above are:

$$l_a \leq \bar{l}_a, \quad \forall a \in L. \tag{3.6}$$

Constraints (3.6) reflect that there is an upper bound on labor associated with each link in the supply chain network.

We now reformulate the objective function of each firm i; $i = 1, \ldots, m$, given by (3.5b) in path flow variables only. We are able to do this because of expressions (3.1), (3.2), (3.3), and (3.4), which, recall, relates labor to product flow. Specifically, we can redefine the total operational cost link functions as: $\tilde{c}_a(x) \equiv \hat{c}_a(f)$, $\forall a \in L$, and the demand price functions as: $\tilde{\rho}_{ik}(x) \equiv \rho_{ik}(d)$, $\forall i$, $\forall k$. Furthermore, as established in Nagurney (2021b), in view of (3.3) and (3.4), we have that: $l_a = \frac{\sum_{p \in P} x_p \delta_{ap}}{\alpha_a}$, for all $a \in L$.

Recall also that, according to Table 1, x^i denotes the vector of strategies, which are the path flows, for each firm i; $i = 1, \ldots, m$. We can redefine the utility/profit functions $\tilde{U}_i(x) \equiv U_i$; $i = 1 \ldots, m$, and group the profits of all the firms into an m-dimensional vector $\tilde{U}$, such that

$$\tilde{U} = \tilde{U}(x). \tag{3.7}$$

Objective function (3.5b), in view of the above, can, thus, be expressed as:

$$\text{Maximize} \quad \tilde{U}_i(x) = \sum_{k=1}^{n_R} \tilde{\rho}_{ik}(x) \sum_{p \in P_k^i} x_p - \sum_{a \in L^i} \tilde{c}_a(x) - \sum_{a \in L^i} \frac{\pi_a}{\alpha_a} \sum_{p \in P} x_p \delta_{ap}. \tag{3.8}$$

Furthermore, it readily follows that constraint (3.6) can be reexpressed exclusively using path flows.

3.2 Governing Equilibrium Conditions and Variational Inequality Formulations

We now state the governing equilibrium conditions for the different scenarios and provide alternative variational inequality formulations for each scenario.

Nash Equilibrium Conditions and Variational Inequality Formulations

We define the feasible set K_i for firm i thus: $K_i \equiv \{x^i | x^i \in R_+^{n_{P^i}}, \frac{\sum_{p \in P^i} x_p \delta_{ap}}{\alpha_a} \leq \bar{l}_a, \forall a \in L^i\}$, for $i = 1, \ldots, m$. Also, we define $K \equiv \prod_{i=1}^m K_i$.

Each firm competes noncooperatively until the following equilibrium is achieved.

Definition 3.1: Supply Chain Network Nash Equilibrium

A path flow pattern $x^* \in K$ *is a supply chain network Nash Equilibrium if for each firm* i*;* $i = 1, \ldots, m$*:*

$$\tilde{U}_i(x^{i*}, \hat{x}^{i*}) \geq \tilde{U}_i(x^i, \hat{x}^{i*}), \quad \forall x^i \in K_i, \tag{3.9}$$

where $\hat{x}^{i*} \equiv (x^{1*}, \ldots, x^{i-1*}, x^{i+1*}, \ldots, x^{m*})$.

According to (3.9), a supply chain Nash Equilibrium is established if no firm can improve upon its profits unilaterally. We know that K is a convex set.

Applying the classical theory of Nash equilibria and variational inequalities, as noted in Section 2 of this tutorial, under our imposed assumptions on the underlying functions, it follows that the solution to the above Nash Equilibrium problem (see Nash (1950, 1951)) coincides with the solution of the variational inequality problem: determine $x^* \in K$, such that

$$-\sum_{i=1}^{m} \langle \nabla_{x^i} \tilde{U}_i(x^*), x^i - x^{i*} \rangle \geq 0, \quad \forall x \in K, \tag{3.10}$$

where $\langle \cdot, \cdot \rangle$ represents the inner product in the corresponding Euclidean space, which here is of dimension n_P, and $\nabla_{x^i} \tilde{U}_i(x)$ is the gradient of $\tilde{U}_i(x)$ with respect to x^i.

Existence of a solution to variational inequality (3.10) is guaranteed since the feasible set K is compact and the utility functions are continuously differentiable, under our imposed assumptions.

We now provide an alternative variational inequality to (3.10) over a simpler feasible set. We introduce Lagrange multipliers λ_a associated with the constraint (3.6) for each link $a \in L$ and group the Lagrange multipliers for each firm i's network L^i into the vector λ^i. We then group all such vectors for the firms into the vector $\lambda \in R^{n_L}_+$. Also, we define the feasible sets: $K^1_i \equiv \{(x^i, \lambda^i) | (x^i, \lambda^i) \in R^{n_{P^i} + n_{L^i}}_+\}$; $i = 1, \ldots, m$, and $K^1 \equiv \prod_{i=1}^m K^1_i$.

Then, using similar arguments as in Theorem 1 in Nagurney, Yu, and Besik (2017), the following result is immediate.

Theorem 3.1: Alternative Variational Inequality Formulation of Nash Equilibrium

The supply chain network Nash Equilibrium satisfying Definition 3.1 is equivalent to the solution of the variational inequality: determine the vector of equilibrium path flows and the vector of optimal Lagrange multipliers, $(x^*, \lambda^*) \in K^1$*, such that:*

$$\sum_{i=1}^{m} \sum_{k=1}^{n_R} \sum_{p \in P^i_k} \left[\frac{\partial \tilde{C}_p(x^*)}{\partial x_p} + \sum_{a \in L^i} \frac{\lambda^*_a}{\alpha_a} \delta_{ap} + \sum_{a \in L^i} \frac{\pi_a}{\alpha_a} \delta_{ap} - \tilde{\rho}_{ik}(x^*) - \sum_{l=1}^{n_R} \frac{\partial \tilde{\rho}_{il}(x^*)}{\partial x_p} \sum_{q \in P^i_l} x^*_q \right] \times [x_p - x^*_p]$$

$$+\sum_{a\in L}\left[\bar{l}_a-\frac{\sum_{p\in P}x_p^*\delta_{ap}}{\alpha_a}\right]\times[\lambda_a-\lambda_a^*]\geq 0,\quad \forall (x,\lambda)\in K^1, \tag{3.11}$$

where for each path p; $p\in P_k^i$; $i=1,\ldots,m$; $k=1,\ldots,n_R$

$$\frac{\partial\tilde{C}_p(x)}{\partial x_p}\equiv\sum_{a\in L^i}\sum_{b\in L^i}\frac{\partial\hat{c}_b(f)}{\partial f_a}, \tag{3.12a}$$

and

$$\frac{\partial\tilde{\rho}_{il}(x)}{\partial x_p}\equiv\frac{\partial\rho_{il}(d)}{\partial d_{ik}}. \tag{3.12b}$$

The above feasible set K^1 is the nonnegative orthant. This feature enables the implementation of an algorithm, which we describe in the next section, which is an iterative procedure that yields closed form expressions at an iteration for the path flows and the link Lagrange multipliers.

Variational inequality (3.11) can be put into standard form (2.1a). We define $X\equiv(x,\lambda)$ and $F(X)\equiv(F^1(X),F^2(X))$, where the p-th component of $F^1(X)$ is given by: $\frac{\partial\tilde{C}_p(x)}{\partial x_p}+\sum_{a\in L^i}\frac{\lambda_a}{\alpha_a}\delta_{ap}+\sum_{a\in L^i}\frac{\pi_a}{\alpha_a}\delta_{ap}-\tilde{\rho}_{ik}(x)-\sum_{l=1}^{n_R}\frac{\partial\tilde{\rho}_{il}(x)}{\partial x_p}\sum_{q\in P_l^i}x_q$, $\forall\in P$, and the b-th component of $F^2(X)$ is given by: $\bar{l}_b-\frac{\sum_{p\in P}x_p\delta_{bp}}{\alpha_b}$, $\forall b\in L$, and where $\mathcal{K}\equiv K^1$, and $N=n_P+n_L$, then, clearly, (3.11) is of the form (2.1a).

3.2 Application of the Modified Projection Method to Solve Numerical Examples

We now, for illustrative purposes, as well as pedagogy, present the Computation Step of the modified projection method (cf. (2.19)) for the solution of variational inequality (3.11) as well as the Adaptation Step (cf. (2.20)).

Realization of the Modified Projection Method Computation Step 2.19 for VI 3.11

Specifically, at iteration τ, we compute each of the path flows $\bar{x}_p^\tau$, $p\in P_k^i$; $i=1,\ldots,m$; $k=1,\ldots,n_R$ according to:

$$\bar{x}_p^\tau=\max\{0,x_p^{\tau-1}-\beta(\frac{\partial\tilde{C}_p(x^{\tau-1})}{\partial x_p}+\sum_{a\in L^i}\frac{\lambda_a^{\tau-1}}{\alpha_a}\delta_{ap}+\sum_{a\in L^i}\frac{\pi_a}{\alpha_a}\delta_{ap}$$
$$-\tilde{\rho}_{ik}(x^{\tau-1})-\sum_{l=1}^{n_R}\frac{\partial\tilde{\rho}_{il}(x^{\tau-1})}{\partial x_p}\sum_{q\in P_l^i}x_q^{\tau-1})\} \tag{3.13}$$

and each of the Lagrange multipliers $\bar{\lambda}_a^\tau$, $\forall a\in L$, according to:

$$\bar{\lambda}_a^\tau=\max\{0,\lambda_a^{\tau-1}-\beta(\bar{l}_a-\frac{\sum_{p\in P}x_p^{\tau-1}\delta_{ap}}{\alpha_a})\}. \tag{3.14}$$

Realization of the Modified Projection Method Computation Step 2.20 for VI 3.11

At iteration τ, we compute each of the path flows x_p^τ, $p \in P_k^i$; $i = 1, \ldots, m$; $k = 1, \ldots, n_R$, according to:

$$x_p^\tau = \max\{0, x_p^{\tau-1} - \beta(\frac{\partial \tilde{C}_p(\bar{x}^\tau)}{\partial x_p} + \sum_{a \in L^i} \frac{\bar{\lambda}_a^\tau}{\alpha_a}\delta_{ap} + \sum_{a \in L^i} \frac{\pi_a}{\alpha_a}\delta_{ap} - \tilde{\rho}_{ik}(\bar{x}^\tau) - \sum_{l=1}^{n_R} \frac{\partial \tilde{\rho}_{il}(\bar{x}^\tau)}{\partial x_p} \sum_{q \in P_l^i} \bar{x}_q^\tau)\} \quad (3.15)$$

and each of the Lagrange multipliers λ_a^τ, $\forall a \in L$, according to:

$$\lambda_a^\tau = \max\{0, \lambda_a^{\tau-1} - \beta(\bar{l}_a - \frac{\sum_{p \in P} \bar{x}_p^\tau \delta_{ap}}{\alpha_a})\}. \quad (3.16)$$

We now provide numerical examples that are inspired by disruptions in migrant labor for the seasonal picking of berries, specifically, the picking of blueberries in the summer of 2020 of the pandemic (see Tully (2020), Russell (2020), and Woolever (2020)). The numerical examples are stylized, but Internet available resources were utilized to obtain relevant blueberry prices and picking data in the United States (see Galinato, Gallardo, and Hong (2016) and howmuchitis.org (2018)). The flow variables are in pounds of blueberries, whereas the prices are in dollars per pound, and labor is in person hours.

The modified projection method was implemented in FORTRAN and a Linux system at the University of Massachusetts Amherst used for the computation of the solutions. The demand for each demand market was initialized at 40 and equally distributed among the paths connecting each demand market from each origin node (firm). The Lagrange multipliers were all initialized to 0. The modified projection method was considered to have converged if the absolute difference of the path flows differed by no more than 10^{-7} and the same for the Lagrange multipliers.

Examples 3.1, 3.2, and 3.3 have the supply chain network topology given in Figure 2. In these examples there are two competing food firms (which are blueberry farms), each with two planting sites (production locations), and with access to a single distribution center. The two food firms can sell their blueberries at two demand markets.

Example 3.1 - Baseline Example

The total operational cost functions for Food Firm 1 on its supply chain network L^1 are:

$$\hat{c}_a(f) = .0006f_a^2, \quad \hat{c}_b(f) = .0007f_b^2, \quad \hat{c}_c(f) = .001f_c^2, \quad \hat{c}_d(f) = .001f_d^2, \quad \hat{c}_e(f) = .002f_e^2,$$

$$\hat{c}_f(f) = .005f_f^2, \quad \hat{c}_g(f) = .005f_g^2.$$

Also, the total operational costs associated with Food Firm 2's supply chain network L^2 are:

$$\hat{c}_h(f) = .00075f_h^2, \quad \hat{c}_i(f) = .0008f_i^2, \quad \hat{c}_j(f) = .0005f_j^2, \quad \hat{c}_k(f) = .0005f_k^2, \quad \hat{c}_l(f) = .0015f_l^2,$$

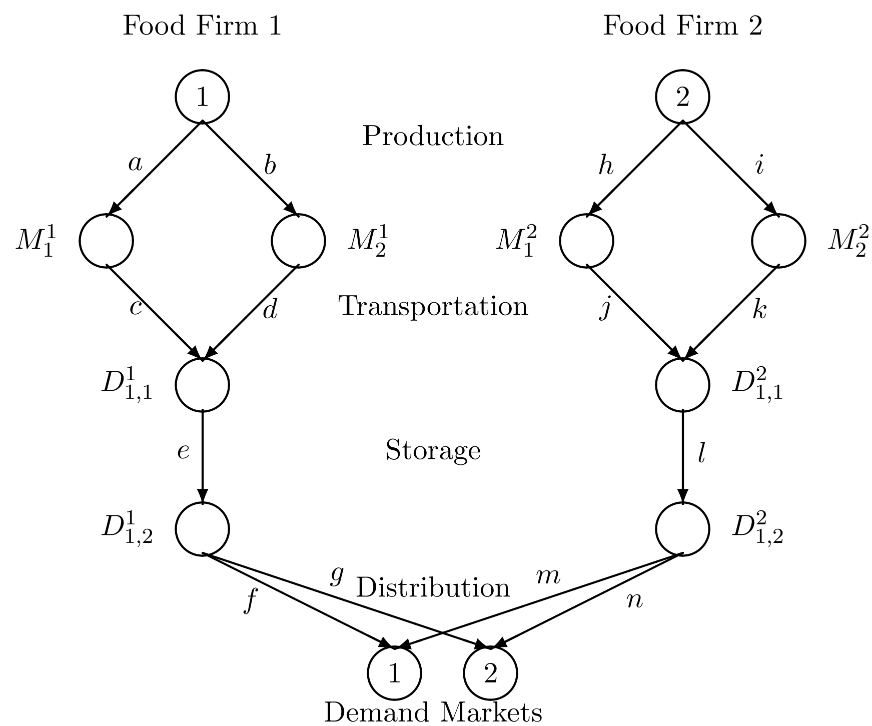

Figure 2: The Supply Chain Network Topology for the Numerical Examples 3.1 Through 3.3

$$\hat{c}_m(f) = .01f_m^2, \quad \hat{c}_n(f) = .01f_n^2.$$

The costs for labor for Food Firm 1 are:

$$\pi_a = 10, \quad \pi_b = 10, \quad \pi_c = 15, \quad \pi_d = 15, \quad \pi_e = 20, \quad \pi_f = 17, \quad \pi_g = 18,$$

and for Food Firm 2:

$$\pi_h = 11, \quad \pi_i = 22, \quad \pi_j = 15, \quad \pi_k = 15, \quad \pi_l = 18, \quad \pi_m = 18, \quad \pi_n = 18.$$

The link labor productivity factors for the first firm are:

$$\alpha_a = 24, \quad \alpha_b = 25, \quad \alpha_c = 100, \quad \alpha_d = 100, \quad \alpha_e = 50, \quad \alpha_f = 100, \quad \alpha_g = 100,$$

and for the second firm:

$$\alpha_h = 23, \quad \alpha_i = 24, \quad \alpha_j = 100, \quad \alpha_k = 100, \quad \alpha_l = 70, \quad \alpha_m = 100, \quad \alpha_n = 100.$$

The bounds on labor for the first firm are:

$$\bar{l}_a = 10, \quad \bar{l}_b = 200, \quad \bar{l}_c = 300, \quad \bar{l}_d = 300, \quad \bar{l}_e = 100, \quad \bar{l}_f = 120, \quad \bar{l}_g = 120,$$

and for the second firm:

$$\bar{l}_h = 800, \quad \bar{l}_i = 90, \quad \bar{l}_j = 200, \quad \bar{l}_k = 200, \quad \bar{l}_l = 300, \quad \bar{l}_m = 100, \quad \bar{l}_n = 100.$$

Observe that the labor availability on link a is low. This is done in order to capture a disruption to labor in the pandemic.

The demand price functions for Food Firm 1 are: $\rho_{11}(d) = -.0001d_{11} - .00005d_{21} + 6$ and $\rho_{12}(d) = -.0002d_{12} - .0001d_{22} + 8$.

The demand price functions for Food Firm 2 are: $\rho_{21}(d) = -.0003d_{21}+7, \quad \rho_{22}(d) = -.0002d_{22}+7$.

The paths are as follows: $p_1 = (a, c, e, f)$, $p_2 = (b, d, e, f)$, $p_3 = (a, c, e, g)$, path $p_r = (b, d, e, g)$, $p_5 = (h, j, l, m)$, $p_6 = (i, k, l, m)$, $p_7 = (h, j, l, n)$, and $p_8 = (i, k, l, n)$.

The modified projection method converges to the path flow equilibrium pattern reported in Table 2; see also the equilibrium link labor values reported in Table 3. All the Lagrange multipliers are equal to 0.00 except for $\lambda_a^* = 4.925$ with the labor equilibrium value on link a equal to its upper bound of 10.00.

The product prices at equilibrium are:

$$\rho_{11} = 5.97, \quad \rho_{12} = 7.91, \quad \rho_{21} = 6.94, \quad \rho_{22} = 6.96,$$

with equilibrium demands of:

$$d_{11}^* = 172.07, \quad d_{12}^* = 359.15, \quad \rho_{21} = 195.94, \quad \rho_{22} = 197.86.$$

The profit of Food Firm 1 is: 1,671.80 and the profit of Food Firm 2 is: 1,145.06.

Example 3.2 – Modification of Demand Price Functions

Example 3.2 has the same data as Example 3.1 except that we modify the demand price functions for the second firm to include a cross term, so that:

$$\rho_{21}(d) = -.0003d_{21} - .0001d_{11} + 6, \quad \rho_{22}(d) = -.0002d_{22} - .0001d_{12} + 7.$$

The computed equilibrium path flows are reported in Table 2, with the computed equilibrium link labor values given in Table 3.

The Lagrange multipliers are all equal to 0.00 except for $\lambda_a^* = 4.93$.

The product prices at equilibrium are now:

$$\rho_{11} = 5.97, \quad \rho_{12} = 7.91, \quad \rho_{21} = 6.92, \quad \rho_{22} = 6.92,$$

with the equilibrium demands:

$$d_{11}^* = 172.07, \quad d_{12}^* = 359.16, \quad d_{21}^* = 195.48, \quad d_{22}^* = 196.48.$$

The profit for Food Firm 1 is: 1,671.86 and the profit for Food Firm 2 is: 1,134.61. The profit for Food Firm 1 rises ever so slightly, whereas that for Food Firm 2 decreases.

Example 3.3 – Disruptions in Storage Facilities

Example 3.3 has the same data as Example 3.2 except that we now consider a sizable disruption in terms of the spread of COVID-19 at the distribution centers of both food firms with the bounds on labor corresponding to the associated respective links being reduced to:

$$\bar{l}_e = 5, \quad \bar{l}_l = 5.$$

The computed equilibrium path flows for this example are reported in Table 2 with Table 3 having the computed equilibrium link labor values for this example, as well.

All computed equilibrium Lagrange multipliers are now equal to 0 except for those associated with the distribution center links, since the equilibrium labor values attain the imposed upper bounds onn links e and l, with the respective equilibrium Lagrange multiplier values being:

$$\lambda_e^* = 157.2138, \quad \lambda_l^* = 43.6537.$$

The product prices at equilibrium are now:

$$\rho_{11} = 5.99, \quad \rho_{12} = 7.94, \quad \rho_{21} = 6.94, \quad \rho_{22} = 6.94,$$

with the equilibrium demands:

$$d_{11}^* = 30.03, \quad d_{12}^* = 219.96, \quad d_{21}^* = 174.61, \quad d_{22}^* = 175.39.$$

The profit for Food Firm 1 is now dramatically reduced to 1,218.74 and the profit for Food Firm 2 also declines, but by a much smaller amount, to 1,126.73.

The above examples illustrate how a rigorous theoretical and computational supply chain network game theory framework with the inclusion of labor can capture different disruptions and also changes to the data.

Table 2: Equilibrium Product Path Flows for Examples 3.1 Through 3.3

Equilibrium Product Path Flows	Ex. 3.1	Ex. 3.2	Ex. 3.3
$x^*_{p_1}$	73.23	73.22	15.65
$x^*_{p_2}$	98.85	98.85	14.38
$x^*_{p_3}$	166.77	166.78	110.60
$x^*_{p_4}$	192.38	192.38	109.35
$x^*_{p_5}$	142.85	142.62	131.97
$x^*_{p_6}$	53.08	52.86	42.63
$x^*_{p_7}$	143.81	143.12	132.36
$x^*_{p_8}$	54.04	53.36	43.02

Table 3: Equilibrium Link Labor Values for Examples 3.1 Through 3.3

Equilibrium Link Labor Values	Ex. 3.1	Ex. 3.2	Ex. 3.3
l^*_a	10.00	10.00	5.26
l^*_b	11.65	11.65	4.95
l^*_c	2.40	2.40	1.26
l^*_d	2.91	2.91	1.24
l^*_e	10.62	10.62	5.00
l^*_f	1.72	1.72	0.30
l^*_g	3.59	3.59	2.20
l^*_h	12.46	12.42	11.49
l^*_i	4.46	4.43	3.57
l^*_j	2.87	2.86	2.64
l^*_k	1.07	1.06	0.86
l^*_l	5.63	5.60	5.00
l^*_m	1.96	1.95	1.75
l^*_n	1.98	1.96	1.75

Example 3.4 – What If There is Only the First Food Firm?

In this example we assume that Food Firm 2 has exited from the supply chain network economy and only Food Firm 1 remains with the data for Food Firm 1 exactly as in Example 3.1, except that there are no cross terms in the demand price functions, since there is no other firm supplying blueberries. The supply chain network topology is, hence, as in Figure 3.

The modified projection method yields the following equilibrium solution. The equilibrium path flow pattern is:

$$x^*_{p_1} = 72.99, \quad x^*_{p_2} = 99.19, \quad x^*_{p_3} = 167.01, \quad x^*_{p_4} = 193.21.$$

The equilibrium link labor values are:

$$l^*_a = 10.00, \quad l^*_b = 11.70, \quad l^*_c = 2.40, \quad l^*_d = 2.92, \quad l^*_e = 10.65, \quad l^*_f = 1.72, \quad l^*_g = 3.60.$$

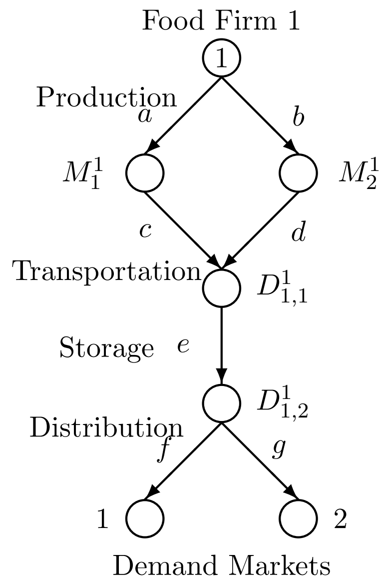

Figure 3: Supply Chain Network Topology for Example 3.4

The Lagrange multipliers are all equal to 0, except for:

$$\lambda_a^* = 5.0253.$$

The demand price at Demand Market 1 is: 5.98 and at Demand Market 2: 7.93 with the computed respective demands being, respectively: 172.18 and: 360.22.

The profit of the firm is: 1,680.61. Since the labor amount is at the bound on link a, the associated Lagrange multiplier is positive. The demand prices at the two demand markets now increase and the profit of Food Firm 1 also increases.

In Nagurney (2021c) additional models with other sets of labor constraints are constructed, which are governed by a Generalized Nash Equilibrium, accompanied by numerical examples. We now turn to game theory and disaster relief supply chains, with a focus on GNE.

4. Disaster Relief Supply Chains

As noted in the Introduction, the COVID-19 pandemic is a healthcare disaster on a global scale. As people became ill, virtually all economic sectors were negatively affected, with supply chain networks disrupted, resulting in fierce competition for many products, including medical supplies, such as PPEs, and, more recently, even vaccines against the coronavirus. In this section, we highlight a Generalized Nash Equilibrium model developed by Nagurney et al. (2021), where additional results can be found. Additional Generalized Nash Equilibrium models, inspired by the COVID-

19 pandemic, and with an eye towards enhanced preparedness and response, along with stochastic elements, can be found in Salarpour and Nagurney (2021). The authors' model is the first stochastic Generalized Nash Equilibrium model for the study of competition among countries for limited supplies of medical items (PPEs, ventilators, etc.) in the disaster preparedness and response phases in the COVID-19 pandemic. Each country's government faces a two-stage stochastic optimization problem in which the first stage is before the pandemic declaration and the second stage is after the pandemic declaration. See also Nagurney et al. (2020b) and the references therein. Therein the authors also considered uncertainty with the consideration of multiple, competing decision-makers in the first Stochastic Generalized Nash Equilibrium model for disaster relief. In their model, there is a single relief item product and the humanitarian organizations compete for existing resources prior to and post the disaster, adjusting their decisions based on the probability of different scenarios. The Nagurney et al. (2020) model integrates logistical and financial features, since humanitarian organizations compete for financial donations, and also freight service, with each one seeking to maximize its expected utility.

4.1 The Generalized Nash Equilibrium Supply Chain Network Model for Medical Supplies Under Stochastic Demand

In the supply chain network model (cf. Figure 4 for the bipartite network structure) there are m supply points for the medical supplies, with a typical supply point denoted by i, and n demand points, with a typical demand point denoted by j. The supply points can be in different regions, states, or even countries. This is of relevance because the competition for PPEs and vaccines has been global in nature. Demand points can be: hospitals, nursing homes, medical clinics, prisons, etc., and even schools, depending on the specific application and medical product. The notation for the model is given in Table 4.

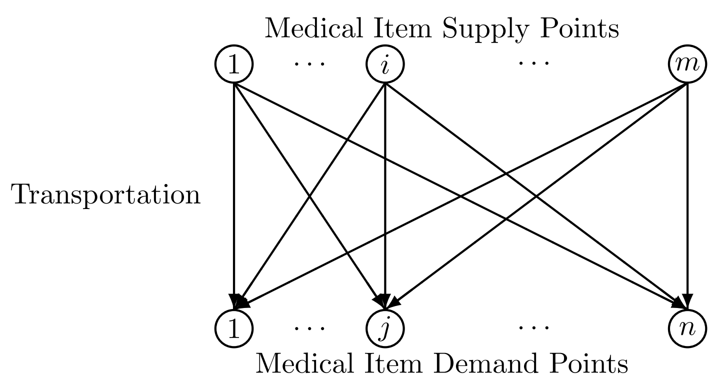

Figure 4: The Network Structure of the Competitive Game Theory Model for Medical Supplies

Table 4: Notation for the Medical Supply Generalized Nash Equilibrium Network Model

Notation	Definition
q_{ij}	the amount of the medical item purchased from supply point i by j. We first group all the i elements $\{q_{ij}\}$ into the vector q_j and then we group such vectors for all j into the vector $q \in R_+^{mn}$.
v_j	the projected demand at demand point j; $j = 1, \ldots, n$.
d_j	the actual (uncertain) demand for the medical item at demand point j; $j = 1, \ldots, n$.
Δ_j^-	the amount of shortage of the medical item at demand point j; $j = 1, \ldots, n$.
Δ_j^+	the amount of surplus of the medical item at demand point j; $j = 1, \ldots, n$.
λ_j^-	the unit penalty associated with a shortage of the medical item at demand point j; $j = 1, \ldots, n$.
λ_j^+	the unit penalty associated with a surplus of the medical item at demand point j; $j = 1, \ldots, n$.
ρ_i	the price of the medical item at supply point i; $i = 1, \ldots, m$.
$c_{ij}(q)$	the generalized cost of transportation associated with transporting the medical item from supply point i to demand point j, which includes the financial cost, relevant tariffs/taxes, time, and risk. We group all the generalized costs into the vector $c(q) \in R^{mn}$.
S_i	the nonnegative amount of the medical item available for purchase at supply point i; $i = 1, \ldots, m$.
μ_i	the nonnegative Lagrange multiplier associated with the supply constraint at supply point i. We group the Lagrange multipliers into the vector $\mu \in R_+^m$.

We emphasize that the demand for the medical product at the demand points is uncertain because of the unpredictability of the actual demand at the demand points. There is a rich supporting literature on supply chain network models with uncertain demand with associated shortage and surplus penalties (see, e.g., Dong, Zhang, and Nagurney (2004), Nagurney, Yu, and Qiang (2011), Nagurney and Masoumi (2012), Nagurney, Masoumi, and Yu (2015)). Nagurney and Nagurney (2016) developed a supply chain network model for disaster relief under cost and demand uncertainty. As noted in Nagurney et al. (2021), the probability distribution of demand for PPEs can be constructed by utilizing census data and/or information gathered during the pandemic disaster preparedness phase.

Some Preliminaries

We now recall some preliminaries, and then discuss the objective functions.

We have that d_j denotes the actual (uncertain) demand at destination point j; hence:

$$P_j(D_j) = P_j(d_j \leq D_j) = \int_0^{D_j} \mathcal{F}_j(t)dt, \qquad j = 1, \ldots, n, \tag{4.1}$$

where P_j and $\mathcal{F}_j$ denote the probability distribution function, and the probability density function of demand at point j, respectively.

The variable v_j is the "projected demand" for the medical item at demand point $j; j = 1, \ldots, n$ and, thus, the amounts of shortage and surplus at demand point j are determined, respectively, as follows:

$$\Delta_j^- \equiv \max\{0, d_j - v_j\}, \qquad j = 1, \ldots, n, \tag{4.2a}$$

$$\Delta_j^+ \equiv \max\{0, v_j - d_j\}, \qquad j = 1, \ldots, n. \tag{4.2b}$$

Moreover, also, as noted in Nagurney et al. (2021), the expected values of shortage and surplus at each demand point are, therefore:

$$E(\Delta_j^-) = \int_{v_j}^{\infty} (t - v_j)\mathcal{F}_j(t)dt, \qquad j = 1, \ldots, n, \tag{4.3a}$$

$$E(\Delta_j^+) = \int_0^{v_j} (v_j - t)\mathcal{F}_j(t)dt, \qquad j = 1, \ldots, n. \tag{4.3b}$$

The expected penalty incurred by demand point j due to the shortage and surplus of the medical item is equal to:

$$E(\lambda_j^- \Delta_j^- \ + \ \lambda_j^+ \Delta_j^+) = \lambda_j^- E(\Delta_j^-) + \lambda_j^+ E(\Delta_j^+), \qquad j = 1, \ldots, n, \tag{4.4}$$

with the weights $\lambda_j^+ + \lambda_j^-$ being greater than zero, for each demand point j. The weight λ_j^- is, typically, significantly higher than the weight λ_j^+ for each j since a shortage of the medical items can be expected to yield greater suffering and loss of life.

The projected demand at demand point j, v_j, is equal to the sum of flows of the medical item to j:

$$v_j \equiv \sum_{i=1}^{m} q_{ij}, \qquad j = 1, \ldots, n. \tag{4.5}$$

Here, we assume that each demand location j, which recall can refer to a hospital, healthcare organization, nursing home, medical facility, etc., seeks to minimize the total costs associated with the purchasing of the medical item plus the total cost of transportation plus the expected cost due to a shortage or surplus at j.

The objective function of each demand point j is, thus:

$$\text{Minimize} \quad \sum_{i=1}^{m} \rho_i q_{ij} + \sum_{i=1}^{m} c_{ij}(q) + \lambda_j^- E(\Delta_j^-) + \lambda_j^+ E(\Delta_j^+) \tag{4.6}$$

subject to:

$$\sum_{j=1}^{n} q_{ij} \leq S_i, \quad i = 1, \ldots, m, \tag{4.7}$$

$$q_{ij} \geq 0, \quad i = 1, \ldots, m. \tag{4.8}$$

Observe that the first term in the objective function (4.6) corresponds to the medical item purchasing costs; the second term corresponds to the generalized total transportation costs; the third term in (4.6) represents the expected cost due to shortage or surplus of the medical item at the demand point j. The constraints (4.7) represent common, that is, shared constraints in that the demand locations compete for the medical items that are available for purchase at the supply locations at a maximum available supply. The constraints in (4.8) correspond to the nonnegativity assumption on the medical item purchase volumes.

We assume that the total generalized transportation cost functions are continuously differentiable and convex. Note that, in our model, the transportation costs can, in general, depend upon the vector of medical item flows since there is competition for freight service provision in the pandemic.

As established in Nagurney et al. (2021), the expected shortage and surplus cost function $\lambda_j^- E(\Delta_j^-) + \lambda_j^+ E(\Delta_j^+)$ is convex.

The objective function (4.6) for j is referred to as the disutility of j and we denote it by $DU_j(q)$; $j = 1, \ldots, n$.

We define the feasible sets $K_j \equiv \{q_j \geq 0\}$; $j = 1, \ldots, n$. We define $K \equiv \prod_{j=1}^{n} K_j$. We also define the feasible set $\mathcal{S} \equiv \{q | q \,\text{satisfying}\, (4.7))\}$, which consists of the shared constraints.

Definition 4.1: Generalized Nash Equilibrium for Medical Items

A vector of medical items $q^* \in K \cap \mathcal{S}$ is a Generalized Nash Equilibrium if for each demand point j; $j = 1, \ldots, n$:

$$DU_j(q_j^*, \hat{q}_j^*) \leq DU_j(q_j, \hat{q}_j^*), \quad \forall q_j \in K_j \cap \mathcal{S}, \tag{4.9}$$

where $\hat{q}_j^* \equiv (q_1^*, \ldots, q_{j-1}^*, q_{j+1}^*, \ldots, q_n^*)$.

According to (4.9), an equilibrium is established if no demand point has any incentive to unilaterally change its vector of medical item purchases/shipments. In this supply chain network model the objective function of a demand point depends not only on the vector of strategies of its own strategies and on those of the other demand points, but the feasible set does as well. Therefore, this supply chain network game theory model is not a Nash (1950, 1951) model, but is a Generalized

Nash Equilibrium model. In the COVID-19 pandemic, the competition has included competition for limited supplies of PPEs, ventilators, associated medical treatments, as well as vaccines.

As noted in Section 2, the concept of a *Variational Equilibrium*, allows us to formulate the above GNE conditions as the solution to a finite-dimensional variational inequality problem. The algorithms for variational inequality problems are at a much more advanced state than are those for quasivariational inequalities, which have been utilized for GNE problems in the past. Indeed, as noted also in Nagurney, Yu, and Besik (2017), in Nagurney, Salarpour, and Daniele (2019), and in Nagurney et al. (2020), we can define a Variational Equilibrium which is a refinement and a specific type of GNE (cf. Kulkarni and Shabhang (2012)) that enables a variational inequality formulation.

Specifically, we now define the feasible set $\mathcal{K} \equiv K \cap \mathcal{S}$.

Definition 4.2: Variational Equilibrium

A vector of medical items $q^* \in \mathcal{K}$ is a Variational Equilibrium of the above Generalized Nash Equilibrium problem if it is a solution to the following variational inequality:

$$\sum_{j=1}^{n}\sum_{i=1}^{m}\frac{\partial DU_j(q^*)}{q_{ij}} \times (q_{ij}-q^*_{ij}) \geq 0, \quad \forall q \in \mathcal{K}. \tag{4.10}$$

The variational inequality (4.10), in expanded form, is: determine $q^* \in \mathcal{K}$ such that

$$\sum_{j=1}^{n}\sum_{i=1}^{m}\left[\rho_i + \sum_{l=1}^{m}\frac{\partial c_{lj}(q^*)}{\partial q_{ij}} + \lambda_j^+ P_j(\sum_{l=1}^{m} q^*_{lj}) - \lambda_j^-(1-P_j(\sum_{l=1}^{m} q^*_{lj}))\right] \times \left[q_{ij}-q^*_{ij}\right] \geq 0, \quad \forall q \in \mathcal{K}. \tag{4.11}$$

We now expand on the interpretation of the above, which is also relevant to disaster relief applications, and, in particular, to the pandemic. The variational equilibrium guarantees that the Lagrange multipliers associated with the shared constraints are identical for all the demand points. This feature provides an elegant fairness and equity interpretation.

Variational inequality (4.11) can be put into standard form (cf. also (2.1a)), where the problem is to determine a vector $X^* \in \mathcal{K} \subset R^N$, such that

$$\langle F(X^*), X - X^* \rangle \geq 0, \quad \forall X \in \mathcal{K}, \tag{4.12}$$

where F is a given continuous function from $\mathcal{K}$ to R^N, and $\mathcal{K}$ is a given closed, convex set.

Let $X \equiv q$ and $F(X)$ be the vector with elements: $\{\frac{\partial DU_j(q^*)}{q_{ij}}\}$, $\forall j, i$ with $\mathcal{K}$ as originally defined and $N = mn$. Then, variational inequality (4.11) can be put into standard form (4.12), under the imposed assumptions.

Since the function $F(X)$ that enters the variational inequality is continuous and the feasible set $\mathcal{K}$ is not only convex but also compact because the supplies of the medical items are bounded, existence of a solution X^* is guaranteed (see Theorem 2.2).

An alternative variational inequality is now provided. We associate a nonnegative Lagrange multiplier μ_i with constraint (4.7), for each supply location $i = 1, \dots, m$ and we group all the Lagrange multipliers into the vector $\mu \in R^m_+$. We define the feasible set $\mathcal{K}^2 \equiv \{(q, \mu) | q \geq 0, \mu \geq 0\}$.

Then, using arguments as in Nagurney, Salarpour, and Daniele (2019), an alternative variational inequality like the one in (4.11) is: determine $(q^*, \mu^*) \in \mathcal{K}^2$ such that

$$\sum_{j=1}^{n}\sum_{i=1}^{m}\left[\rho_i + \sum_{l=1}^{m}\frac{\partial c_{lj}(q^*)}{\partial q_{ij}} + \lambda_j^+ P_j(\sum_{l=1}^{m} q^*_{lj}) - \lambda_j^-(1 - P_j(\sum_{l=1}^{m} q^*_{lj}) + \mu^*_i\right] \times \left[q_{ij} - q^*_{ij}\right]$$

$$+\sum_{i=1}^{m}\left[S_i - \sum_{j=1}^{n} q^*_{ij}\right] \times [\mu_i - \mu^*_i] \geq 0, \quad \forall (q, \mu) \in \mathcal{K}^2. \tag{4.13}$$

Variational inequality (4.13) can also be put into standard form (4.12). Let $X \equiv (q, \mu)$ and $F(X) \equiv (F^1(X), F^2(X))$ where $F^1(X)$ has as its (i, j)-th component: $\rho_i + \sum_{l=1}^{m} \frac{\partial c_{lj}(q)}{\partial q_{ij}} + \lambda_j^+ P_j(\sum_{l=1}^{m} q_{lj}) - \lambda_j^-(1 - P_j(\sum_{l=1}^{m} q_{lj}) + \mu_i$; $i = 1, \dots, m$; $j = 1, \dots, n$, and the i-th component of $F^2(X)$ is $S_i - \sum_{j=1}^{n} q_{ij}$, for $i = 1, \dots, m$. Furthermore, $\mathcal{K} \equiv \mathcal{K}^2$ and $N = mn + m$.

4.2 Computation of Numerical Examples

We emphasize that additional theoretical results can be found in Nagurney et al. (2021). We now provide the realization of the modified projection method (cf. Section 2) for the solution of the above alternative variational inequality problem.

We now provide the explicit formulae for the medical item flows and the Lagrange multipliers at iteration τ for Step 1. The analogues for Step 2 can be easily derived accordingly.

Specifically, we have the following formulae:

Explicit Formula for the Medical Item Flow for Each i, j at Iteration τ of Step 1

Determine $\bar{q}^\tau_{ij}$ for each i, j at Step 1 iteration τ according to:

$$\bar{q}^\tau_{ij} = \max\{0, q^{\tau-1}_{ij} + \beta(-\rho_i - \sum_{l=1}^{m}\frac{\partial c_{lj}(q^{\tau-1})}{\partial q_{ij}} - \lambda_j^+ P_j(\sum_{l=1}^{m} q^{\tau-1}_{lj}) + \lambda_j^-(1 - P_j(\sum_{l=1}^{m} q^{\tau-1}_{lj})) - \mu^{\tau-1}_i)\}. \tag{4.14}$$

Explicit Formula for the Lagrange Multiplier for Each i at Iteration τ of Step 1

Determine $\bar{\mu}_i^\tau$ for each i at Step 1 iteration τ according to:

$$\bar{\mu}_i^\tau = \max\{0, \mu_i^{\tau-1} + \beta(-S_i + \sum_{j=1}^{n} q_{ij}^{\tau-1})\}. \tag{4.15}$$

The modified projection method was implemented in FORTRAN and the computer system used was a Linux system at the University of Massachusetts Amherst. The algorithm was initialized by setting the medical item flows and the Lagrange multipliers to 0.00. The convergence condition for all the examples was that the absolute value of two successive variable iterates was less than or equal to 10^{-8}. The β parameter in the modified projection method was: .1.

The numerical examples (with additional ones reported in Nagurney et al. (2021)) are focused on the procurement of N95 masks but in the scenario of increasing demand among smaller healthcare organizations in the form of medical practices. The q_{ij}s are in units since these medical practices are small relative to hospitals, etc. Please see the following news article by O'Connell (2020) and also Wan (2020).

Example 4.1: One Supply Point and Two Demand Points

The supply chain network topology for this example is given in Figure 5. We assume a uniform probability distribution in the range $[100, 1000]$ at the first demand point. The probability distribution at the second demand point has the same lower and upper bounds as in the first demand point. The additional data are, for the first demand point:

$$\rho_1 = 2, \quad S_1 = 1000, \quad c_{11}(q) = .005q_{11}^2 + .01q_{11}, \quad \lambda_1^- = 1000, \quad \lambda_1^+ = 10,$$

and for the second demand point:

$$c_{12}(q) = .01q_{12}^2 + .02, \quad \lambda_2^- = 1000, \quad \lambda_2^+ = 10.$$

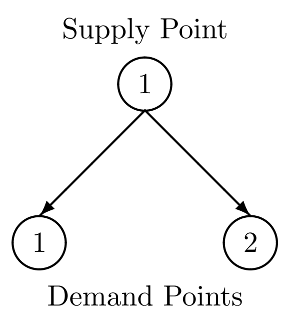

Figure 5: Supply Chain Network Topology for Example 4.1

The modified projection method converges to the following equilibrium solution:

$$q_{11}^* = 502.20, \quad q_{12}^* = 497.80, \quad \mu_1^* = 541.61.$$

The available supply of 1000 N95 masks is exhausted between the two demand points, and the associated Lagrange multiplier μ_1^* is positive. The equilibrium conditions hold with excellent accuracy.

Example 4.2: Two Supply Points and Two Demand Points

In Example 4.2, we consider the impacts of the addition of a second supply point to Example 4.1. The supply chain network topology is now as in Figure 6.

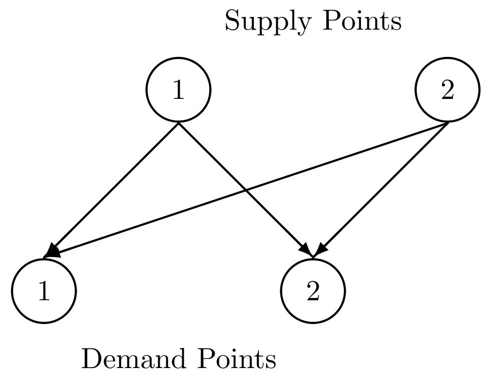

Figure 6: Supply Chain Network Topology for Example 4.2

The data are as in Example 4.1 with the following additions:

$$S_2 = 500, \quad \rho_2 = 3, \quad c_{21}(q) = .015q_{21}^2 + .03, \quad c_{22}(q) = .02q_{22}^2 + .04q_{22}.$$

The modified projection method converges to the following equilibrium solution:

$$q_{11}^* = 526.31, \quad q_{12}^* = 473.69, \quad q_{21}^* = 225.57, \quad q_{22}^* = 274.43, \quad \mu_1^* = 261.17, \quad \mu_2^* = 258.65.$$

With the addition of a new supply point for medical supplies, both demand points gain significantly in terms of the volume of N95 masks that each procure, Furthermore, the supplies of the medical item at each supply point are fully sold out. Hence, both equilibrium Lagrange multipliers are positive.

Example 4.3: Two Supply Points and Three Demand Points

Example 4.3 is constructed from Example 4.2 with Demand Point 3 added, as depicted in Figure 7.

Example 4.3 has the same data as Example 4.2 but with the addition of data for Demand Point 3 as follows:

$$c_{13}(q) = .01q_{13}^2 + .02q_{13}, \quad c_{23}(q) = .015q_{23}^2 + .03q_{23}, \quad \lambda_3^- = 1000, \quad \lambda_3^+ = 10.$$

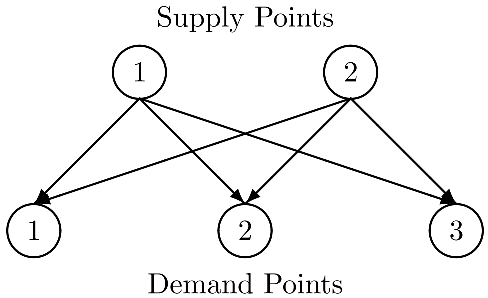

Figure 7: Supply Chain Network Topology for Example 4.3

The probability distribution for the N95 masks associated with Demand Point 3 is uniform with a lower bound of 200 and an upper bound of 1000.

The modified projection method converges to the following equilibrium solution:

$$q_{11}^* = 360.11, \quad q_{12}^* = 318.83, \quad q_{13}^* = 321.06,$$

$$q_{21}^* = 122.29, \quad q_{22}^* = 161.10, \quad q_{23}^* = 216.62, \quad \mu_1^* = 565.25, \quad \mu_2^* = 564.16.$$

Note that, with increasing competition for the N95 masks with another demand point, both Demand Points 1 and 2 experience decreases in procurement of supplies. The two supply points again fully sell out of their N95 masks and the associated equilibrium Lagrange multipliers are both positive.

Example 4.4: Two Supply Points and Four Demand Points

In Example 4.4, yet another demand point is added to the supply chain network topology of Example 4.3 (cf. Figure 8). Smaller medical practices are increasingly concerned about being able to secure the much needed PPEs to protect the health of their employees and the viability of their practices.

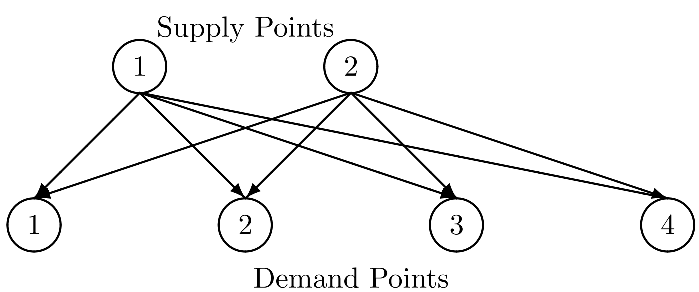

Figure 8: Supply Chain Network Topology for Example 4.4

The data for this example are the same as those for Example 4.3, and the probability distribution structure for the demand at Demand Point 4 is the same, with the following additional data for the new Demand Point 4:

$$c_{14}(q) = .015q_{14}^2 + .03q_{14}, \quad c_{24}(q) = .025q_{24}^2 + .05q_{24}, \quad \lambda_4^- = 1000, \quad \lambda_4^+ = 10.$$

The modified projection method converges to the following equilibrium solution:

$$q_{11}^* = 260.73, \quad q_{12}^* = 229.36, \quad q_{13}^* = 251.22, \quad q_{14}^* = 258.69,$$

$$q_{21}^* = 79.57, \quad q_{22}^* = 109.17, \quad q_{23}^* = 160.46, \quad q_{24}^* = 150.81, \quad \mu_1^* = 725.71, \quad \mu_2^* = 724.91.$$

As noted in Nagurney et al. (2021) the equilibrium conditions hold with excellent accuracy for this example, as was the case for all the other numerical example computed solutions. The suppliers of the N95 sell out their supplies. However, the demand points lose in terms of supply procurement for their organizations with the increased demand and competition from yet another demand point. We emphasize that the obtained numerical results are consistent with what is being observed in practice and the results also provide managerial insights. For example, the numerical results confirm that more supply points with sufficient supplies are needed to guarantee that organizations are not deprived of critical supplies due to competition. As a result of this competition and limited local availability, in particular in the case of supplies such as masks, ventilators, and even coronavirus test kits, we are seeing multiple countries now setting up local production sites with even some companies switching from their usual product manufacturing to the production of much needed medical supplies, including PPEs (Bradsher (2020)).

5. Cooperation in Disaster Relief

In Sections 3 and 4 the focus was on noncooperative game theory and supply chain network models inspired by the COVID-19 pandemic, with the model in Section 3 providing a commercial supply chain network framework, and with the inclusion of labor, and with the model in Section 4 being one representing organizations competing for medical supplies, which have been limited, in the pandemic. Here, in contrast, we turn to cooperation among organizations in a disaster setting. As emphasized in Nagurney and Qiang (2020), opportunities for cooperation among organizations engaged in disaster response may exist in their supply chains from procurement to storage and even in the case of transportation and distribution (see Van Wassenhove (2006), Nagurney and Qiang (2009), Balcik et al. (2010), among others). Furthermore, cooperation among organizations may reduce materiel convergence and release resources, including personne, for more important life-saving tasks (cf. Nagurney, Alvarez Flores, and Soylu (2016)). There is also great promise in the COVID-19 pandemic of enhanced partnerships and these even may be between private companies, including pharmaceutical ones (Hopkins (2021)). Lessons learned from disaster management are, hence, potentially of great benefit to pandemic preparedness, response, and even recovery.

Here we highlight how to quantify synergies due to cooperation associated with multiproduct supply chains of multiple organizations, engaged in disaster response, including the COVID-19 pandemic. The models, due to Nagurney and Qiang (2020), capture the uncertainties associated with costs and demands. A mean-variance approach is used to include risk associated with the uncertainties, along with a synergy measure for the determination of the potential strategic advantages of cooperation among organizations for disaster management.

Nagurney and Qiang (2009), earlier, described how the multiproduct supply chain network models of Nagurney, Woolley, and Qiang (2010) could be used to measure the synergy associated with teaming in the form of horizontal cooperation between humanitarian organizations. Masoumi, Yu, and Nagurney (2017), later, constructed several synergy measures to evaluate the mergers or acquisitions associated with multiple blood banks in the United States, which are, typically, nonprofits. Their blood supply chain network models pre- and post- the merger/acquisition were generalized, nonlinear networks in order to capture the perishability of blood. Toyasaki et al. (2017), noting horizontal cooperation for inventory management, and practiced by the United Nations Humanitarian Response Depot (UNHRD) network, built an analytical framework to identify horizontal cooperation for such management between humanitarian organizations.

5.1 The Multiproduct Supply Chain Network Models

Section 5.1.1 describes the underlying supply chain network associated with multiple, individual organizations without horizontal cooperation and their associated economic activities of procurement, transportation, storage, and distribution. Section 5.1.2 presents the supply chain network model with horizontal cooperation. The models extend those of Nagurney (2009), Nagurney, Woolley, and Qiang (2010), Nagurney and Nagurney (2016), and Masoumi, Yu, and Nagurney (2017) to multiproduct supply chains of multiple organizations, with uncertainties in both costs and demands, and upper bounds on links.

5.1.1 The Case without Horizontal Cooperation Multiproduct Supply Chain Network Model

We first formulate the multiproduct decision-making optimization problems faced by m organizations without horizontal cooperation. This model is Case 0. Each organization is represented as a network of its supply chain activities, as depicted in Figure 9. Each organization i; $i = 1, \ldots, m$, has available n^i_M procurement facilities, n^i_S storage facilities, and serves n^i_D disaster areas. Let

$G_i = [N_i, L_i]$ denote the graph consisting of nodes $[N_i]$ and directed links $[L_i]$ representing the supply chain activities associated with each organization i; $i = 1, \ldots, m$. Let L^0 denote the links: $L_1 \cup L_2 \cup \cdots L_m$ as in Figure 9. Each organization is involved in the procurement, transportation, storage, and distribution of J products, with a typical product denoted by j.

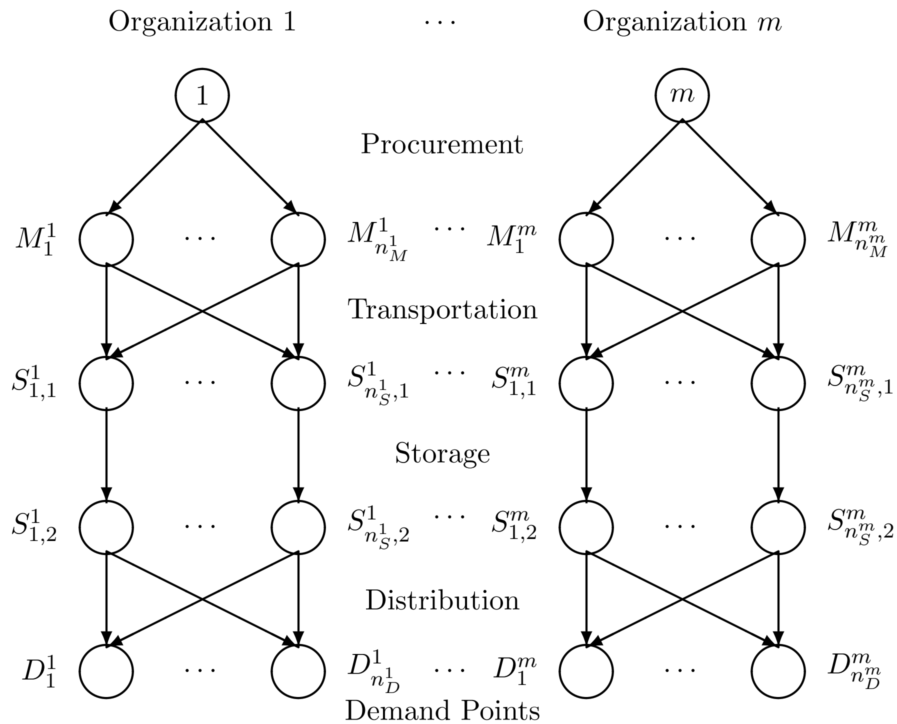

Figure 9: Supply Chains of Organizations 1 through m Prior to Cooperation

The links from the top-tiered nodes i; $i = 1, \ldots, m$, in each supply chain network in Figure 9 are connected to the procurement nodes of the respective organization i, which are denoted, respectively, by: $M_1^i, \ldots, M_{n_M^i}^i$ and are the procurement links. The links from the procurement nodes are joined to the storage center nodes of each organization i; $i = 1, \ldots, m$, and are denoted by $S_{1,1}^i, \ldots, S_{n_S^i,1}^i$. These links represent the transportation links between the procurement facilities and the storage centers. Links connecting nodes $S_{1,1}^i, \ldots, S_{n_S^i,1}^i$ with nodes $S_{1,2}^i, \ldots, S_{n_S^i,2}^i$ for $i = 1, \ldots, m$, are the storage links for the products. Also, there are distribution links connecting nodes $S_{1,2}^i, \ldots, S_{n_S^i,2}^i$ for $i = 1, \ldots, m$ with the disaster region nodes: $D_1^i, \ldots, D_{n_D^i}^i$ for each organization $i = 1, \ldots, m$. These are the demand points. Each organization i is responsible for providing the products to specific disaster areas (see Figure 9), prior to the cooperation, for the victims.

The notation and discussion below build upon those in Section 4. Specifically, demands for the products are assumed to be random and are associated with each product, and each demand point. Let d_{ik}^j denote the random variable representing the actual demand for product j and let v_{ik}^j denote the projected random demand for product j; $j = 1, \ldots, J$, at demand point D_k^i for

$i = 1, \ldots, m$; $k = 1, \ldots, n^i_D$. In addition, the probability density function of the actual demand for product j is $\mathcal{F}^j_{ik}(t)$ at disaster area D^i_k; $i = 1, \ldots, m$; $k = 1, \ldots, n^i_D$. Hence, we can define the cumulative probability distribution function of d^j_{ik} as $\mathcal{P}^j_{ik}(v^j_{ik}) = \mathcal{P}^j_{ik}(d^j_{ik} \leq v^j_{ik}) = \int_0^{v^j_{ik}} \mathcal{F}^j_{ik}(t)d(t)$. Following Masoumi, Yu, and Nagurney (2017) and Dong, Zhang, and Nagurney (2004), we also define the supply shortage and surplus for product j; $j = 1, \ldots, J$, at disaster area D^i_k; $i = 1, \ldots, m$; $k = 1, \ldots, n^i_D$, as

$$\Delta^{j-}_{ik} \equiv \Delta^{j-}_{ik}(v^j_{ik}) \equiv \max\{0, d^j_{ik} - v^j_{ik}\} \tag{5.1a}$$

$$\Delta^{j+}_{ik} \equiv \Delta^{j+}_{ik}(v^j_{ik}) \equiv \max\{0, v^j_{ik} - d^j_{ik}\}. \tag{5.1b}$$

The expected value of the shortage Δ^{j-}_{ik}, denoted by $E(\Delta^{j-}_{ik})$, and of the surplus Δ^{j+}_{ik}, denoted by $E(\Delta^{j+}_{ik})$, for $j = 1, \ldots, J$; D^i_k; $i = 1, \ldots, m$; $k = 1, \ldots, n^i_D$, are

$$E(\Delta^{j-}_{ik}) = \int_{v^j_{ik}}^{\infty} (t - v^j_{ik})\mathcal{F}^j_{ik}(t)d(t), \quad E(\Delta^{j+}_{ik}) = \int_0^{v^j_{ik}} (v^j_{ik} - t)\mathcal{F}^j_{ik}(t)d(t). \tag{5.2}$$

The penalty associated with the shortage and the surplus of the demand for product j; $j = 1, \ldots, J$, at the disaster area D^i_k is denoted by λ^{j-}_{ik} and λ^{j+}_{ik}, respectively, where $i = 1, \ldots, m$; $k = 1, \ldots, n^i_D$.

A path consists of a sequence of links originating at a node i; $i = 1, \ldots, m$, corresponding to supply chain activities of: procurement, transportation, storage, and distribution of the products to the disaster area nodes. We let x^j_p denote the nonnegative flow of product j on path p. Let $P^0_{D^i_k}$ denote the set of all paths joining an origin node i with (destination) disaster area node D^i_k. The paths associated with a given organization, prior to a possible cooperation, share no links with paths of the other organization. This feature is no longer the case (see also Nagurney (2009) and Masoumi, Yu, and Nagurney (2017)) once cooperation happens. Then, as we will show, the number of paths as well as the sets of paths change, as do the number of links and the sets of links, as described in Section 5.1.2. The conservation of flow equations are: for each organization $i; i = 1, \ldots, m$, each product $j; j = 1, \ldots, J$, and each disaster area $D^i_k; k = 1, \ldots, n^i_D$:

$$\sum_{p \in P^0_{D^i_k}} x^j_p = v^j_{ik}, \quad i = 1, ..., m; \quad j = 1, \ldots, J; \quad k = 1, \ldots, n^i_D. \tag{5.3}$$

In other words, the projected demand for each disaster relief product associated with a humanitarian organization at a demand point must be satisfied by the sum of the product path flows of the organization's supply chain network.

Links are denoted by a, b, etc. Let f^j_a denote the flow of product j on link a. We also have the following conservation of flow equations:

$$f_a^j = \sum_{p \in P^0} x_p^j \delta_{ap}, \quad j = 1 \ldots, J; \quad \forall a \in L^0, \tag{5.4}$$

where $\delta_{ap} = 1$ if link a is contained in path p and $\delta_{ap} = 0$, otherwise. Here P^0 denotes the set of *all* paths in Figure 1, that is, $P^0 = \cup_{i=1,\ldots,I;k=1,\ldots,n_D^i} P^0_{D_k^i}$. The path flows must be nonnegative, that is,

$$x_p^j \geq 0, \quad j = 1, \ldots, J; \quad \forall p \in P^0. \tag{5.5}$$

The path flows are grouped into the vector x.

There is a total cost associated with each product j; $j = 1, \ldots, J$, and each link of the network of each organization i; $i = 1, \ldots, m$. The total cost on a link a associated with product j is denoted by $\hat{c}_a^j$. The total cost of a link associated with a product, be it a procurement link, a transportation/distribution link, or a storage link can be, for the sake of generality, a function of the flow of all the products on the link. Furthermore, the total costs can be influenced by uncertainty factors. Hence, the total cost on link a, $\hat{c}_a^j$, takes the form:

$$\hat{c}_a^j = \hat{c}_a^j(f_a^1, \ldots, f_a^J, \omega_a^j), \quad j = 1, \ldots, J; \quad \forall a \in L^i, \forall i, \tag{5.6}$$

where ω_a^j is a random variable associated with various disaster events, which have an impact on the total cost of link a, $\forall a$, and product j; $j = 1, \ldots, J$. It is assumed that the distribution of the ω_a^js is known.

As stated in Nagurney and Qiang (2020), the top tier links in Figure 9 have associated with them multiproduct total cost functions that capture the purchasing/procurement costs of the products. The links comprising the second tier links have associated with them multiproduct total cost functions that capture the total costs associated with the transportation to the storage facilities. The third tier links have associated with them multiproduct total cost functions that reflect storage costs. The bottom-tiered links have total cost functions associated with them that capture the distribution costs.

It is important to emphasize that the supply chain networks of the organizations, as depicted in Figure 9, include the prepositioning of the relief items in the preparedness phase of disaster management, through the storage links, plus the distribution of the relief items via the distribution links in the response phase.

Building on the earlier literature utilizing a mean-variance approach, the organizations consider both costs and risks in their operations with each organization seeking to minimize its expected total cost and the valuation of its risk. Moreover, since the organizations' supply chains without horizontal cooperation have no links or costs in common (cf. Figure 9), the optimization problems of the organizations are independent prior to the possible cooperation. Each organization i; $i = 1, \ldots, m$ seeks to determine the link flows and the projected random demands that solve the following optimization problem:

$$\text{Minimize} \quad \Bigg[E(\sum_{j=1}^{J} \sum_{a \in L_i} \hat{c}_a^j(f_a^1, \ldots, f_a^J, \omega_a^j)) + \xi_i (V(\sum_{j=1}^{J} \sum_{a \in L_i} \hat{c}_a^j(f_a^1, \ldots, f_a^J, \omega_a^j)))$$

$$+ \sum_{j=1}^{J} \sum_{k=1}^{n_D^i} \big(\lambda_{ik}^{j-} E(\Delta_{ik}^{j-}) + \lambda_{ik}^{j+} E(\Delta_{ik}^{j+}) \big) \Bigg] \tag{5.7}$$

subject to: constraints (5.3) – (5.5) and the following capacity constraints:

$$\sum_{j=1}^{J} \gamma_j f_a^j \leq u_a, \quad \forall a \in L_i. \tag{5.8}$$

The term γ_j in (5.8) reflects the volume taken up by product j; the term u_a is the nonnegative capacity of link a.

The first and the second terms in (5.7) are the expected total cost of organization i and the variance of the total cost, respectively, with the term ξ_i being the risk aversion factor of organization i. $V(\sum_{j=1}^{J} \sum_{a \in L_i} \hat{c}_a^j(f_a^1, \ldots, f_a^J, \omega_a^j))$ denotes the variance of the total cost of organization i. The third term in (5.7) is the total costs related to the shortage and/or surplus of the relief items at the disaster areas that i is responsible for. The total operational costs and the variances in (5.7) are assumed to be convex. As argued in Section 4, we know that $\sum_{k=1}^{n_D^i} \big(\lambda_{ik}^{j-} E(\Delta_{ik}^{j-}) + \lambda_{ik}^{j+} E(\Delta_{ik}^{j+}) \big)$ is also convex (see, also, Nagurney, Masoumi, and Yu (2012)). We know then that the objective function (5.7) is convex for each i; $i = 1, \ldots, m$. Also, the individual terms in (5.7) are continuously differentiable. Under the above imposed assumptions, the optimization problem is a convex optimization problem and, clearly, the feasible set underlying the problem represented by the constraints (5.3) – (5.5) and (5.8) is non-empty, so it follows from the standard theory of nonlinear programming that an optimal solution exists.

The objective function (5.7) is referred to as the total generalized cost TGC_i^0 for $i = 1, \ldots, m$. We associate the Lagrange multiplier η_a with constraint (5.8) for each $a \in L^0$ with $\eta_a \geq 0, \forall a \in L^0$ and we denote the associated optimal Lagrange multiplier by $\eta_a^*, \forall a \in L^0$. We group the link flows into the vector f, the projected demands into the vector v, and the Lagrange multipliers into the vector η.

Let $\mathcal{K}^0$ denote the set where $\mathcal{K}^0 \equiv \{(f, v, \eta) | \exists x \, \text{such that} \, (5.3) - (5.5) \, \text{and} \, \eta \geq 0 \, \text{hold}\}$. We now provide the variational inequality formulation of the problem (5.7) for all organizations i;

$i = 1, \ldots, m$, simultaneously. Since we are considering Case 0, we denote the solution of variational inequality (VI) (5.9) below as $(f^{0*}, v^{0*}, \eta^{0*})$ and we refer to the corresponding vectors of variables with superscripts of 0. We now state a theorem, due to Nagurney and Qiang (2020).

Theorem 5.1: Variational Inequality Formulation of Case 0: No Cooperation

The vector of link flows, projected demands, and Lagrange multipliers $(f^{0*}, v^{0*}, \eta^{0*}) \in \mathcal{K}^0$ is an optimal solution to (5.7), for all organizations i; $i = 1, \ldots, m$, subject to their constraints (5.3)–(5.5) and (5.8), if and only if it satisfies the following variational inequality problem:

$$\sum_{i=1}^{m}\sum_{j=1}^{J}\sum_{a\in L_i}[\frac{\partial E(\sum_{l=1}^{J}\sum_{a\in L_i}\hat{c}_a^l(f_a^{1*},\ldots,f_a^{J*},\omega_a^l))}{\partial f_a^j}$$

$$+\xi_i\frac{\partial V(\sum_{l=1}^{J}\sum_{a\in L_i}\hat{c}_a^l(f_a^{1*},\ldots,f_a^{J*},\omega_a^l))}{\partial f_a^j}+\gamma_j\eta_a^*]\times[f_a^j-f_a^{j*}]$$

$$+\sum_{i=1}^{m}\sum_{j=1}^{J}\sum_{k=1}^{n_D^i}\left[\lambda_{ik}^{j+}\mathcal{P}_{ik}^j(v_{ik}^{j*})-\lambda_{ik}^{j-}(1-\mathcal{P}_{ik}^j(v_{ik}^{j*})\right]\times[v_{ik}^j-v_{ik}^{j*}]$$

$$+\sum_{a\in L^0}[u_a-\sum_{j=1}^{J}\gamma_j f_a^{j*}]\times[\eta_a-\eta_a^*]\geq 0,\quad \forall(f^0,v^0,\eta^0)\in\mathcal{K}^0. \tag{5.9}$$

5.1.2 The Case with Horizontal Cooperation Multiproduct Supply Chain Network Model

We now formulate the case with horizontal cooperation of the multiproduct supply chain network model, referred to as Case 1. Figure 10 represents the supply chain network topology for Case 1. There is a *supersource* node 0, which represents the "teaming/merging" in terms of cooperation of the organizations in terms of their supply chain networks with additional links connecting node 0 to nodes 1 through m.

The optimization problem in Case 1 is also concerned with cost and risk minimization. We refer to the network in Figure 10, underlying this integration, as $G^1 = [N^1, L^1]$ where $N^1 \equiv N^0 \cup$ node 0 and $L^1 \equiv L^0 \cup$ the additional links as in Figure 10 and we associate total cost functions as in (5.6) with the new links, for each product j. If the total cost functions on the cooperation links connecting node 0 to node 1 through node m are set equal to zero, this means that the cooperation is *costless* in terms of the integrated supply chain network of the organizations.

A path p now (cf. Figure 10) originates at node 0 and ends in one of the bottom disaster nodes. Let x_p^j, under the cooperation network configuration given in Figure 9, denote the flow of product

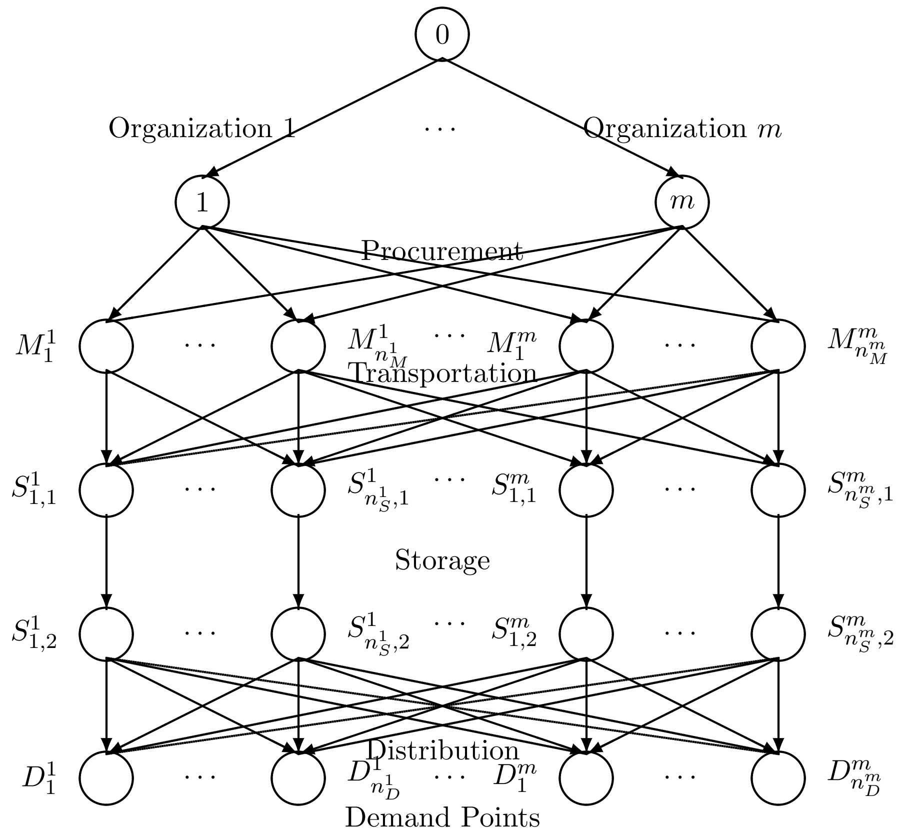

Figure 10: Supply Chain Network after Cooperation

j on path p joining (origin) node 0 with a disaster area node. Then, the following conservation of flow equations must hold for each i, j, k:

$$\sum_{p \in P^1_{D^i_k}} x^j_p = v^j_{ik}, \tag{5.10}$$

where $P^1_{D^i_k}$ denotes the set of paths connecting node 0 with disaster area node D^i_k in Figure 10. Because of cooperation, the disaster areas can obtain each product j from any procurement facility, and any storage facility. The set of paths $P^1 \equiv \cup_{i=1,m;k=1,\ldots,n^i_D} P^1_{D^i_k}$.

As previously, let f^j_a denote the flow of product j on link a. We must also have the following conservation of flow equations satisfied:

$$f^j_a = \sum_{p \in P^1} x^j_p \delta_{ap}, \quad j = 1, \ldots, J; \quad \forall a \in L^1. \tag{5.11}$$

In addition, the path flows must be nonnegative for each product j:

$$x^j_p \geq 0, \quad j = 1, \ldots, J; \quad \forall p \in P^1. \tag{5.12}$$

The supply chain network activities have nonnegative capacities, denoted as u_a, $\forall a \in L^1$, with γ_j representing the volume factor for product j. The following constraints must, hence, hold:

$$\sum_{j=1}^{J} \gamma_j f_a^j \leq u_a, \quad \forall a \in L^1, \tag{5.13}$$

where ξ is the associated risk aversion factor of the teamed organizations under cooperation.

The optimization problem for the teamed supply chain network is:

$$\text{Minimize} \quad E(\sum_{j=1}^{J} \sum_{a \in L^1} \hat{c}_a^j(f_a^1, \ldots, f_a^J, \omega_a^j)) + \xi \left[V(\sum_{j=1}^{J} \sum_{a \in L^1} \hat{c}_a^j(f_a^1, \ldots, f_a^J, \omega_a^j)) \right]$$

$$+ \sum_{i=1}^{m} \sum_{j=1}^{J} \sum_{k=1}^{n_D^i} \left(\lambda_{ik}^{j-} E(\Delta_{ik}^{j-}) + \lambda_{ik}^{j+} E(\Delta_{ik}^{j+}) \right) \tag{5.14}$$

subject: (5.10) – (5.13).

The solution to the optimization problem (5.14) subject to constraints (5.10), for all i, j, k, through (5.13) can also be obtained as a solution to a variational inequality problem, similar to (5.9), where now links $a \in L^1$. The vectors f, v, and η retain their prior definitions, but are re-dimensioned accordingly and superscripted with 1. Finally, instead of the feasible set $\mathcal{K}^0$ we now have $\mathcal{K}^1 \equiv \{(f, v, \eta) | \exists x \, \text{such that} \, (5.10) - (5.12) \, \text{hold and} \, \eta \geq 0\}$.

For consistency, objective function (5.14) is referred to as the total generalized cost TGC^1.

We denote the solution to the variational inequality (VI) problem (5.15) below governing Case 1 by $(f^{1*}, v^{1^*}, \eta^{1*})$ and denote the vectors of corresponding variables as (f^1, v^1, η^1). The proof of the following is immediate.

Theorem 5.2: Variational Inequality Formulation of Case 1: Cooperation

The vector of link flows, projected demands, and Lagrange multipliers $(f^{1*}, v^{1*}, \eta^{1*}) \in \mathcal{K}^1$ is an optimal solution to (5.14), subject to constraints (5.10)–(5.13), if and only if it satisfies the following variational inequality problem:

$$\sum_{j=1}^{J} \sum_{a \in L^1} [\frac{\partial E(\sum_{l=1}^{J} \sum_{a \in L^1} \hat{c}_a^l(f_a^1, \ldots, f_a^J, \omega_a^l))}{\partial f_a^j} + \xi \frac{\partial V(\sum_{l=1}^{J} \sum_{a \in L^1} \hat{c}_a^l(f_a^{1*}, \ldots, f_a^{J*}, \omega_a^l))}{\partial f_a^j} + \gamma_j \eta_a^*]$$

$$\times [f_a^j - f_a^{j*}] + \sum_{i=1}^{m} \sum_{j=1}^{J} \sum_{k=1}^{n_D^i} \left[\lambda_{ik}^{j+} \mathcal{P}_{ik}^j(v_{ik}^{j*}) - \lambda_{ik}^{j-}(1 - \mathcal{P}_{ik}^j(v_{ik}^{j*}) \right] \times [v_{ik}^j - v_{ik}^{j*}]$$

$$+ \sum_{a \in L^1} [u_a - \sum_{j=1}^{J} \gamma_j f_a^{j*}] \times [\eta_a - \eta_a^*] \geq 0, \quad \forall (f^1, v^1, \eta^1) \in \mathcal{K}^1. \tag{5.15}$$

Definition 5.1: Total Generalized Costs at the Optimal Solutions to the Supply Chain Network Problems without and with Cooperation

Let TGC^{0*} *denote the total generalized cost:* $\sum_i^m TGC_i^0 = E(\sum_{j=1}^J \sum_{a\in L^0} \hat{c}_a^j(f_a^1,\ldots,f_a^J,\omega_a^j)) + \sum_{i=1}^m \xi_i \Big[V(\sum_{j=1}^J \sum_a$
$\lambda_{ik}^{j+}E(\Delta_{ik}^{j+})\big)$*, evaluated at the optimal solution* $(f^{0*}, v^{0*}, \eta^{0*})$ *to (5.9).*

Also, let $TGC^{1*} = E(\sum_{j=1}^J \sum_{a\in L^1} \hat{c}_a^j(f_a^1,\ldots,f_a^J,\omega_a^j)) + \xi \Big[V(\sum_{j=1}^J \sum_{a\in L^1} \hat{c}_a^j(f_a^1,\ldots,f_a^J,\omega_a^j))\Big]$
$+\sum_{i=1}^m \sum_{j=1}^J \sum_{k=1}^{n_D^i} \big(\lambda_{ik}^{j-}E(\Delta_{ik}^{j-}) + \lambda_{ik}^{j+}E(\Delta_{ik}^{j+})\big)$*, denote the total generalized cost evaluated at the solution* $(f^{1*}, v^{1*}, \eta^{1*})$ *to (5.15).*

5.2 Synergy Quantification

We now quantify the synergy associated with cooperation of the organizations by analyzing the total generalized costs under the cases with and without supply chain network cooperation.

We denote the synergy by $\mathcal{S}^{TGC}$. It is the percentage difference between the total generalized cost without *vs.* with the horizontal cooperation (evaluated at the respective optimal solutions):

$$\mathcal{S}^{TGC} \equiv [\frac{TGC^{0*} - TGC^{1*}}{TGC^{0*}}] \times 100\%. \tag{5.16}$$

Observe from (5.16) that the lower the total generalized cost TGC^{1*}, the higher the synergy associated with the supply chain network cooperation and, therefore, the greater the total cost savings resulting from the cooperation. As noted in Nagurney and Qiang (2020), the general costs include not only the monetary costs, but also the risks and uncertainties involved in the supply chain as well as the associated penalties of shortages and surpluses. In specific disaster relief operations, including in the pandemic, one may evaluate the integration of supply chain networks with only a subset of the links connecting the original supply chain networks. Figure 10 would be then be adapted accordingly and the synergy as in (5.16) computed with TGC^{1*} corresponding to the specific supply chain network topology.

We now recall an interesting theorem, due also to Nagurney and Qiang (2020), which reveals that, under certain assumptions related to the total operational costs associated with the supply chain integration and risk factors, the associated synergy can never be negative.

Theorem 5.3

If the total generalized cost functions associated with the cooperation links from node 0 *to nodes* 1 *through* m *for each product are identically equal to zero, and if the risk aversion factors* ξ_i*;* $i = 1, \ldots, m$*, are all equal and set to* ξ*, then the associated synergy,* $\mathcal{S}^{TGC}$*, can never be negative.*

As emphasized in Nagurney and Qiang (2020), because of the conservation of flow equations (5.10) and (5.11), and constraints (5.12) and (5.13), we can construct a variational inequality formulation equivalent to the one in (5.15), but in path flows, rather than in links flows (the same holds for a path flow version of VI (5.9)). The alternative variational inequality enables a nice application of the modified projection method.

We group the path flows into the vector $x \in R^{n_{P^1}}$, where n_{P^1} is the number of paths in P^1. We let n_{L^1} denote the number of links in L^1.

We define the feasible set $\mathcal{K}^2 \equiv \{(x, \eta) | x \geq 0, \eta \geq 0\}$. Then the VI (5.17) below follows directly from the relationships between variational inequalities and nonlinear programming problems (cf. Nagurney (1999) and the references therein) (or, equivalently, by utilizing the conservation of flow expressions and embedding them into the link flow VI analogue (5.15), along with algebraic simplification). A vector of path flows and Lagrange multipliers $(x^*, \eta^*) \in \mathcal{K}^2$ is an optimal solution to problem (5.14) subject to (5.10) – (5.13) if and only if it satisfies the variational inequality:

$$\sum_{j=1}^{J} \sum_{p \in P^1} \left[\frac{\partial TGC^1(x^*)}{\partial x_p^j} + \gamma_j \sum_{a \in L^1} \eta_a^* \delta_{ap} \right] \times \left[x_p^j - x_p^{j*} \right]$$

$$+ \sum_{a \in L^1} \left[u_a - \sum_{j=1}^{J} \gamma_j \sum_{p \in P^1} x_p^{j*} \delta_{ap} \right] \times [\eta_a - \eta_a^*] \geq 0, \quad \forall (x, \eta) \in \mathcal{K}^2. \tag{5.17}$$

Variational inequality (5.17) can be put into standard form (2.1a). Let $X \equiv (x, \eta)$ and $F(X) \equiv (F_1(X), F_2(X))$, where $F_1(X)$ consists of elements: $\left[\frac{\partial TGC^1(x)}{\partial x_p^j} + \gamma_j \sum_{a \in L^1} \eta_a \delta_{ap} \right]$, $\forall j, \forall p \in P^1$, and $F_2(X)$ of elements: $\left[u_a - \sum_{j=1}^{J} \gamma_j \sum_{p \in P^1} x_p^j \delta_{ap} \right]$, $\forall a \in L^1$. Then, clearly, (5.17) can be put into the form (2.1a), where $N = n_{P^1} + n_{L^1}$.

5.3 Numerical Examples

The numerical examples are inspired, in part, by ongoing refugee/migrant crises as in Central America and Mexico (cf. Stemple (2019)), which are ongoing and have been exacerbated in the COVID-19 pandemic (see Nagurney, Daniele, and Cappello (2021)). Slow-onset, ongoing disasters are providing huge challenges for various organizations, including humanitarian ones, and governments, to provide the necessary food, water, medicines, etc., to the needy in a variety of shelters. The numerical examples are stylized but reflect real-world features. Furthermore, as in the case of the refugee/migrant crisis emanating from Central America, numerous organizations are involved in providing assistance and, hence, it is valuable to be able to assess possible synergies since the demand is so great. Using carefully calibrated historical data and information, the models can be used to assist the organizations on how to cooperate in terms of the delivery of relief products in a cost-effective manner.

The pre-cooperation supply chain network for the numerical examples is depicted in Figure 11 and the cooperation one in Figure 12.

According to Figure 11, there are two organizations, Organization 1 and Organization 2, each of which is to provide relief items to disaster victims at two demand points. The demand points associated with Organization 1, D_1^1 and D_2^1, differ from those of Organization 2, that is, D_1^2 and D_2^2.

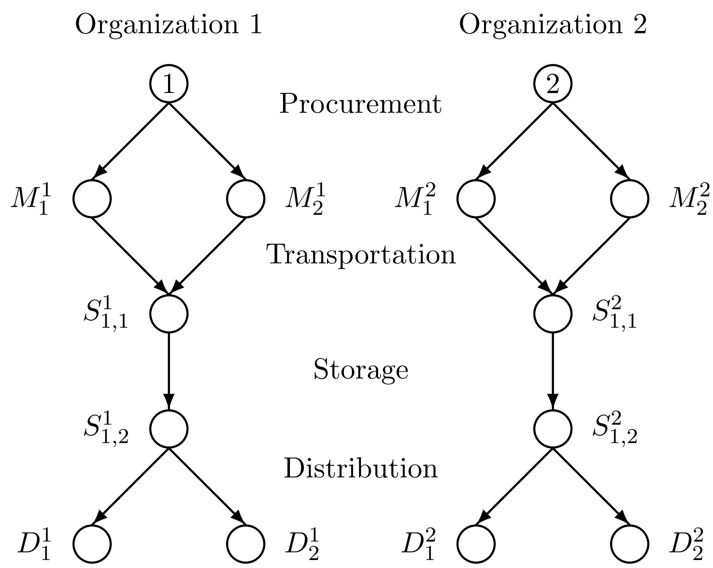

Figure 11: Pre-Cooperation Supply Chain Network Topology for the Numerical Examples

Pre-cooperation, each organization can procure the relief items from two possible locations (distinct for each organization) and then have the items transported for storage to a separate storage facility, from which the relief items are ultimately transported to the points of demand. On the other hand, under cooperation, as the supply chain network in Figure 11 reveals, the demand points can be serviced by either organization (or both), and they can make use of one another's storage facilities as well as freight services for transportation and distribution, and can also avail themselves of all the procurement location options.

In the numerical examples, we consider a single product and, thus, we suppress the superscripts associated with products in our notation.

The total link cost functions are of the form:

$$\hat{c}_a = c_a(f_a, \omega_a) = \omega_a \hat{g}_a f_a + g_a f_a, \quad \forall a \in L^1.$$

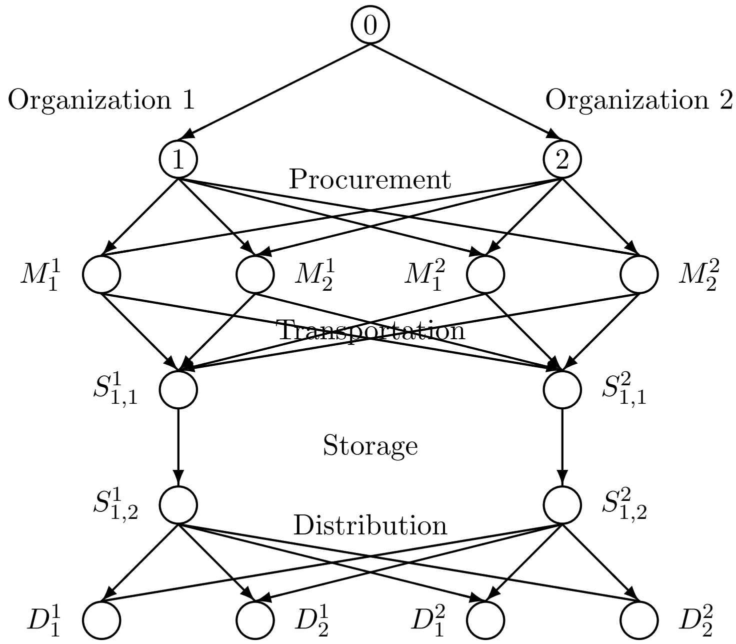

Figure 12: Cooperation Supply Chain Network Topology for the Examples

The objective function (5.14) takes the form:

$$\text{Minimize} \quad \sum_{a\in L^1} E(\omega_a)\hat{g}_a f_a + \sum_{a\in L^1} g_a f_a + \xi V(\sum_{a\in L^1} \omega_a \hat{g}_a f_a) + \sum_{i=1}^{m}\sum_{k=1}^{n_D^i}\big(\lambda_{ik}^- E(\Delta_{ik}^-) + \lambda_{ik}^+ E(\Delta_{ik}^+)\big), \quad (5.18)$$

where in the examples $m = 2$.

The covariance matrix associated with the $\hat{c}_a(f_a, \omega_a)$, $\forall a \in L^1$, is the 28×28 matrix $\sigma^2 I$, since there are 28 links in the network in Figure 12.

Following Nagurney and Nagurney (2016), we know that:

$$\sum_{a\in L^1} \sigma^2 \hat{g}_a^2 f_a^2 = V(\sum_{a\in L^1} \omega_a \hat{g}_a f_a) = V(\sum_{a\in L^1} \omega_a \hat{g}_a \sum_{q\in\mathcal{P}} x_q \delta_{aq}); \quad (5.19)$$

hence,

$$\frac{\partial V(\sum_{a\in L^1} \omega_a \hat{g}_a \sum_{q\in\mathcal{P}} x_q \delta_{aq})}{\partial x_p} = 2\sigma^2 \sum_{a\in L^1} \hat{g}_a^2 f_a \delta_{ap}. \quad (5.20)$$

We define the following marginal total cost on a link a, $\hat{G}c_a'$, as:

$$G\hat{c}_a' \equiv E(\omega_a)\hat{g}_a + g_a + \xi 2\sigma^2 \hat{g}_a^2 f_a, \quad (5.21)$$

and the following marginal total cost on a path:

$$G\hat{C}_p' \equiv \sum_{a\in L^1} G\hat{c}_a' \delta_{ap}, \quad \forall p \in P^1. \quad (5.22)$$

For both the pre-cooperation model and the cooperation model, Steps 1 and 2 of the modified projection method (cf. (2.19) and (2.20)) result in closed form expressions for the product path flows as well as the Lagrange multipliers at each iteration. Below we provide the associated explicit formulae for Step 1 for the solution of VI (5.17). Analogous formulae are easily obtained for Step 2.

Closed Form Expressions for the Product Path Flows and the Lagrange Multipliers at Step 1 of Iteration τ

The closed form expression for the product path flow $\bar{x_p^j}^{\tau}$ for each $p \in P^1$; $j = 1, \ldots, J$, at iteration τ is:

$$\bar{x_p^j}^{\tau} = \max\{0, \beta \left[-\frac{\partial TGC^1(x^{\tau-1})}{\partial x_p^j} - \gamma_j \sum_{a \in L^1} \eta_a^{\tau-1} \delta_{ap} \right] + {x_p^j}^{\tau-1}\}. \tag{5.23}$$

The closed form expression for the Lagrange multiplier $\bar{\eta}_a^{\tau}$ for $a \in L^1$ is:

$$\bar{\eta}_a^{\tau} = \max\{0, \beta \left[\sum_{j=1}^{J} \gamma_j \sum_{p \in P^1} {x_p^j}^{\tau-1} \delta_{ap} - u_a \right] + \eta_a^{\tau-1}\}. \tag{5.24}$$

Note that $\frac{\partial TGC^1(x^{\tau-1})}{\partial x_p}$ in the algorithmic statement (5.23) would take the form (cf. Masoumi, Yu, and Nagurney (2017)), $\forall i$, $\forall k$, $\forall p \in P^1_{D^i_k}$:

$$\frac{\partial TGC^1(x^{\tau-1})}{\partial x_p} = G\hat{C}'_p(x^{\tau-1}) - \lambda_{ik}^{-}(1 - \mathcal{P}_{ik}(\sum_{q \in P^1_{D^i_k}} x_q^{\tau-1})) + \lambda_{ik}^{+} \mathcal{P}_{ik}(\sum_{q \in P^1_{D^i_k}} x_q^{\tau-1}). \tag{5.25}$$

We implemented the algorithm in FORTRAN and utilized a Linux system at the University of Massachusetts Amherst for the computations. The algorithm was initialized with the projected demand for each demand point set to 100 and equally distributed among the paths. The convergence tolerance ϵ was set to 10^{-5}; that is, the algorithm was terminated when the absolute value of the difference of successive path flows at two iterations as well as that of successively computed Lagrange multipliers were all less than or equal to this ϵ value.

Example 5.1

The definitions of the links, the upper bounds on the links, and the associated total link cost functions are given in Table 5 for Example 5.1. Example 5.2 is constructed from Example 5.1. It has the same data except for the probability distribution functions at the demand points. The time horizon under consideration is one week.

Since we assume one type of relief item, we set (cf. (5.8)) $\gamma_1 = 1$. The product to be delivered to the shelters is that of relief item kits, so our costs/prices associated with the procurement links (cf. Table 5) are reasonable (cf. Nagurney, Salarpour, and Daniele (2019)). The weights $\xi_1 = \xi_2 = 1$ apply for the without cooperation supply chain network problem (cf. Figure 11).

The demand at each of the four demand points in Figures 11 and 12 for Example 5.1 is assumed to follow a continuous uniform distribution on the intervals: $[150, 400]$, $[150, 250]$, $[150, 500]$, and $[100, 200]$, respectively. Hence, the demand at the second demand point of each HO is lower than at its first demand location. We then have that, for Organization 1:

$$\mathcal{P}_{11}(\sum_{p \in P^0_{D^1_1}} x_p) = \frac{\sum_{p \in P^0_{D^1_1}} x_p - 150}{400 - 150}, \quad \mathcal{P}_{12}(\sum_{p \in P^0_{D^1_2}} x_p) = \frac{\sum_{p \in P^0_{D^1_2}} x_p - 150}{250 - 150},$$

and, for Organization 2:

$$\mathcal{P}_{21}(\sum_{p \in P^0_{D^2_1}} x_p) = \frac{\sum_{p \in P^0_{D^2_1}} x_p - 150}{500 - 150}, \quad \mathcal{P}_{22}(\sum_{p \in P^0_{D^2_2}} x_p) = \frac{\sum_{p \in P^0_{D^2_2}} x_p - 100}{200 - 100}.$$

The demand points associated with Organization 1 are in the western part of a region, whereas those associated with Organization 2 are in the eastern part. Their respective storage centers are located centrally.

We set $\sigma^2 = 1$. For the construction of the $G\hat{c}'_a$, $\forall a \in L^1$, please refer to equation (5.21) and Table 5.

Also, we set: $\lambda^-_{ik} = 10000$ and $\lambda^+_{ik} = 100$ for both organizations and all demand points since shortages are penalized more than surpluses.

The computed optimal link flows and Lagrange multipliers for this example, prior to cooperation, are reported in Table 6.

The component of the total generalized cost TGC^{0*} not including the penalized expected shortages and surpluses is equal to $1,415,963$, whereas the total generalized cost $TGC^{0*} = 1,024,443,264$.

As can be seen from the results in Table 6, the volume of relief item flows into each demand point is above the minimum amount of the corresponding interval of the associated probability distribution. Interestingly, the relief item flows on the procurement links of both organizations are at their respective link capacities and, hence, the corresponding optimal Lagrange multipliers are positive. The organizations may wish to discuss with their suppliers the possibility of procuring additional items in the future.

Table 5: Definition of Links, the Link Upper Bounds, and Associated Total Cost and Other Functions for Examples 5.1 and 5.2

Link a	From Node	To Node	u_a	$\hat{c}_a(f_a,\omega_a)=\omega_a\hat{g}_a f_a + g_a f_a$	$E(\omega_a)$	$G\hat{c}'_a$
1	1	M_1^1	200	$\omega_1 2f_1 + 60f_1$	1	$8f_1 + 62$
2	1	M_2^1	175	$\omega_2 f_2 + 55f_2$	1	$2f_2 + 56$
3	M_1^1	$S_{1,1}^1$	250	$\omega_3 f_3 + 4f_3$	1	$2f_3 + 5$
4	M_2^1	$S_{1,1}^1$	200	$\omega_4 f_4 + 5f_4$	1	$2f_4 + 6$
5	$S_{1,1}^1$	$S_{1,2}^1$	400	$\omega_5 f_5 + 2f_5$	1	$2f_5 + 3$
6	$S_{1,2}^1$	D_1^1	300	$\omega_6 2f_6 + 2f_6$	1	$8f_6 + 4$
7	$S_{1,2}^1$	D_2^1	300	$\omega_7 2f_7 + 2f_7$	1	$8f_7 + 4$
8	2	M_1^2	175	$\omega_8 f_8 + 50f_8$	1	$2f_8 + 51$
9	2	M_2^2	175	$\omega_9 f_9 + 45f_9$	1	$2f_9 + 46$
10	M_1^2	$S_{1,1}^2$	300	$\omega_{10} f_{10} + 2f_{10}$	1	$2f_{10} + 3$
11	M_2^2	$S_{1,1}^2$	300	$\omega_{11} f_{11} + 6f_{11}$	1	$2f_{11} + 7$
12	$S_{1,1}^2$	$S_{1,2}^2$	450	$\omega_{12} 2f_{12} + 2f_{12}$	1	$8f_{12} + 4$
13	$S_{1,2}^2$	D_1^2	350	$\omega_{13} f_{13} + 7f_{13}$	1	$2f_{13} + 8$
14	$S_{1,2}^2$	D_2^2	200	$\omega_{14} f_{14} + 8f_{14}$	1	$2f_{14} + 9$
15	1	M_1^2	150	$\omega_{15} f_{15} + 50f_{15}$	1	$2f_{15} + 51$
16	1	M_2^1	175	$\omega_{16} f_{16} + 45f_{16}$	1	$2f_{16} + 46$
17	2	M_1^1	175	$\omega_{17} 2f_{17} + 60f_{17}$	1	$8f_{17} + 62$
18	2	M_2^1	150	$\omega_{18} f_{18} + 55f_{18}$	1	$2f_{18} + 56$
19	M_1^1	$S_{1,1}^2$	200	$\omega_{19} f_{19} + 5f_{19}$	1	$2f_{19} + 6$
20	M_2^1	$S_{1,1}^2$	200	$\omega_{20} f_{20} + 6f_{20}$	1	$2f_{20} + 7$
21	M_1^2	$S_{1,1}^1$	200	$\omega_{21} f_{21} + 3f_{21}$	1	$2f_{21} + 4$
22	M_2^2	$S_{1,1}^1$	200	$\omega_{22} f_{22} + 7f_{22}$	1	$2f_{22} + 8$
23	$S_{1,2}^1$	D_1^2	200	$\omega_{23} 2f_{23} + 3f_{23}$	1	$8f_{23} + 5$
24	$S_{1,2}^1$	D_2^2	200	$\omega_{24} 2f_{24} + 3f_{24}$	1	$8f_{24} + 5$
25	$S_{1,2}^2$	D_1^1	150	$\omega_{25} f_{25} + 8f_{25}$	1	$2f_{25} + 9$
26	$S_{1,2}^2$	D_2^1	150	$\omega_{26} f_{26} + 9f_{26}$	1	$2f_{26} + 10$
27	0	1	large	0	–	0
28	0	2	large	0	–	0

In Table 7, we report the computed optimal solution for the cooperation supply chain network for Example 5.1. We set $\xi = 1$.

Again, the relief item flows to the demand points are all greater than the lower value of the interval of the respective probability distribution. Moreover, whereas in the case without cooperation, a total of 725 relief items were delivered across all demand points, now 850 have been delivered under cooperation. Hence, victims benefit from the cooperation of organizations.

In the optimal solution to the supply chain network with cooperation, as reported in Table 7, the relief item flows at the two storage locations are now at capacity levels, as is the flow on

Table 6: Optimal Link Flows and Lagrange Multipliers for Examples 5.1 and 5.2 without Cooperation

			Example 5.1		Example 5.2	
Link a	From Node	To Node	f_a^*	η_a^*	f_a^*	η_a^*
1	1	M_1^1	200	3448	200	1878
2	1	M_2^1	175	4753	175	3183
3	M_1^1	$S_{1,1}^1$	200	0	200	0
4	M_2^1	$S_{1,1}^1$	175	0	175	0
5	$S_{1,1}^1$	$S_{1,2}^1$	375	0	375	0
6	$S_{1,2}^1$	D_1^1	202	0	187.5	0
7	$S_{1,2}^1$	D_2^1	173	0	187.5	0
8	2	M_1^2	175	3774	175	1026
9	2	M_2^2	175	3775	175	1027
10	M_1^2	$S_{1,1}^2$	175	0	175	0
11	M_2^2	$S_{1,1}^2$	175	0	175	0
12	$S_{1,1}^2$	$S_{1,2}^2$	350	0	350	0
13	$S_{1,2}^2$	D_1^2	226	0	200	0
14	$S_{1,2}^2$	D_2^2	124	0	150	0

the shipment link from the second storage facility to the fourth (last) demand point. Hence, the Lagrange multipliers associated with these links (links 5, 12, and 26) are now positive.

The component of the total generalized cost TGC^{1*}, not including the penalized expected shortages and surpluses, is equal to $1,480,565$, whereas the total generalized cost $TGC^{1*} = 466,333,824$.

The resulting synergy for Example 5.1, associated with cooperation, is, hence, $\mathcal{S}^{TGC} = 54\%$. The organizations also gain under cooperation, in addition to the refugees.

Example 5.2

Example 5.2 has the identical data to that in Example 5.1 except that we assume that there are now better estimates of the demand ranges for the first and third demand points. We now have that, for Organization 1:

$$\mathcal{P}_{11}(\sum_{p\in P^0_{D_1^1}} x_p) = \frac{\sum_{p\in P^0_{D_1^1}} x_p - 150}{250-150},$$

and for Organization 2:

$$\mathcal{P}_{21}(\sum_{p\in P^0_{D_1^2}} x_p) = \frac{\sum_{p\in P^0_{D_1^2}} x_p - 150}{250-150}.$$

Table 7: Optimal Link Flows and Lagrange Multipliers for Examples 5.1 and 5.2 with Cooperation

			Example 5.1		Example 5.2	
Link a	From Node	To Node	f_a^*	η_a^*	f_a^*	η_a^*
1	1	M_1^1	86	0	106	0
2	1	M_2^1	112	0	106	0
3	M_1^1	$S_{1,1}^1$	78.5	0	100	0
4	M_2^1	$S_{1,1}^1$	106	0	100	0
5	$S_{1,1}^1$	$S_{1,2}^1$	400	7291	400	11305
6	$S_{1,2}^1$	D_1^1	79.5	0	110	0
7	$S_{1,2}^1$	D_2^1	140	0	110	0
8	2	M_1^2	114	0	106	0
9	2	M_2^2	114	0	106	0
10	M_1^2	$S_{1,1}^2$	120	0	113	0
11	M_2^2	$S_{1,1}^2$	120	0	113	0
12	$S_{1,1}^2$	$S_{1,2}^2$	450	4917	450	9737
13	$S_{1,2}^2$	D_1^2	96	0	123	0
14	$S_{1,2}^2$	D_2^2	115	0	82	0
15	1	M_1^2	114	0	106	0
16	1	M_2^1	114	0	106	0
17	2	M_1^1	86	0	106	0
18	2	M_2^1	112	0	106	0
19	M_1^1	$S_{1,1}^2$	93.5	0	113	0
20	M_2^1	$S_{1,1}^2$	117	0	113	0
21	M_1^2	$S_{1,1}^1$	108	0	100	0
22	M_2^2	$S_{1,1}^1$	108	0	100	0
23	$S_{1,2}^1$	D_1^2	81	0	100	0
24	$S_{1,2}^1$	D_2^2	100	0	70	0
25	$S_{1,2}^2$	D_1^1	90	0	123	0
26	$S_{1,2}^2$	D_2^1	150	703	123	0
27	0	1	425	0	425	0
28	0	2	425	0	425	0

The computed optimal solution for the supply chain network for Example 5.2 without cooperation is reported in Table 6 and that for the supply chain network with cooperation is reported in Table 7.

In Example 5.2, the same links in the without cooperation supply chain network are at their capacities, in terms of the link flows, as in Example 5.1; that is, the procurement links. Also, in the case of cooperation, the storage links are at their capacities in both Examples 5.1 and 5.2, whereas link 26, corresponding to a shipment/distribution link, is only at its capacity in Example 5.1 and not in Example 5.2.

The component of the total generalized cost TGC^{0*}, not including the penalized expected shortages and surpluses, is equal to $1,409,139$, whereas the total generalized cost $TGC^{0*} = 494,335,328$. The component of the total generalized cost TGC^{1*}, not including the penalized expected shortages and surpluses, is equal to 1,498,029, whereas the total generalized cost $TGC^{1*} = 1,536,779$.

The resulting synergy associated with cooperation for Example 5.2 has $\mathcal{S}^{TGC} = 99\%$. With tighter estimates of the projected demand, a higher generalized total cost synergy is achieved. The needy now receive volumes of relief kits closer to the higher bound of the respective interval over which the probability distribution function is defined.

Example 5.3

In Example 5.3, we consider the situation where Organization 1 is in a developed country with access to more resources, whereas Organization 2 is in a developing country with fewer resources, and is also more susceptible/exposed to natural disasters and strife, with a greater number of victims requiring shelters.

The data for Example 5.3 are as in Example 5.2 except for the following: the capacities on certain procurement links were increased so that:

$$u_1 = 400, u_2 = 350, \quad u_7 = 350, u_8 = 350.$$

Also, in order to reflect that Organization 1 has access to greater resources, the capacity on its storage link (link 5) was increased, so that now

$$u_5 = 600.$$

$\mathcal{P}_{11}$ and $\mathcal{P}_{12}$ remain as in Example 5.2, but, in order to consider higher demand at demand points originally associated with Organization 2 (cf. Figure 12) in Example 5.3 we have now that:

$$\mathcal{P}_{21}(\sum_{p \in P^0_{D^2_1}} x_p) = \frac{\sum_{p \in P^0_{D^2_1}} x_p - 400}{500 - 400},$$

and

$$\mathcal{P}_{22}(\sum_{p \in P^0_{D^2_2}} x_p) = \frac{\sum_{p \in P^0_{D^2_2}} x_p - 300}{400 - 300}.$$

The computed optimal solution for this example without cooperation is reported in Table 8, and that for this example with cooperation, in Table 9.

The component of the total generalized cost TGC^{0*}, not including the penalized expected shortages and surpluses, is equal to $1,974,112$ whereas the total generalized cost $TGC^{0*} = 2,574,611,712$.

Table 8: Optimal Link Flows and Lagrange Multipliers for Example 5.3 without Cooperation

			Example 5.3	
Link a	From Node	To Node	f_a^*	η_a^*
1	1	M_1^1	207	0
2	1	M_2^1	200	0
3	M_1^1	$S_{1,1}^1$	207	0
4	M_2^1	$S_{1,1}^1$	200	1276
5	$S_{1,1}^1$	$S_{1,2}^1$	407	0
6	$S_{1,2}^1$	D_1^1	204	0
7	$S_{1,2}^1$	D_2^1	204	0
8	2	M_1^2	225.4	0
9	2	M_2^2	225.6	0
10	M_1^2	$S_{1,1}^2$	225	0
11	M_2^2	$S_{1,1}^2$	225	0
12	$S_{1,1}^2$	$S_{1,2}^2$	450	17549
13	$S_{1,2}^2$	D_1^2	274	0
14	$S_{1,2}^2$	D_2^2	176	0

Whereas in Example 5.2 the total volume of delivered relief items was 850; in Example 5.3 the total volume is $1,050$.

In Example 5.3, under cooperation, both organizations utilize the storage facilities to their capacities.

The component of the total generalized cost TGC^{1*}, not including the penalized expected shortages and surpluses, is equal to 2,108,016 whereas the total generalized cost $TGC^{1*} = 2,255,516$.

The synergy $\mathcal{S}^{TGC}$ is again 99%, showing the potential benefits of cooperation among organizations for disaster relief, including in the COVID-19 pandemic.

Table 9: Optimal Link Flows and Lagrange Multipliers for Example 5.3 with Cooperation

			Example 5.3	
Link a	From Node	To Node	f_a^*	η_a^*
1	1	M_1^1	131	0
2	1	M_2^1	131	0
3	M_1^1	$S_{1,1}^1$	150	0
4	M_2^1	$S_{1,1}^1$	150	0
5	$S_{1,1}^1$	$S_{1,2}^1$	600	12652
6	$S_{1,2}^1$	D_1^1	99	0
7	$S_{1,2}^1$	D_2^1	99	0
8	2	M_1^2	131	0
9	2	M_2^2	131	0
10	M_1^2	$S_{1,1}^2$	113	0
11	M_2^2	$S_{1,1}^2$	113	0
12	$S_{1,1}^2$	$S_{1,2}^2$	450	21084
13	$S_{1,2}^2$	D_1^2	234	0
14	$S_{1,2}^2$	D_2^2	153	0
15	1	M_1^2	131	0
16	1	M_2^1	131	0
17	2	M_1^1	131	0
18	2	M_2^1	131	0
19	M_1^1	$S_{1,1}^2$	113	0
20	M_2^1	$S_{1,1}^2$	113	0
21	M_1^2	$S_{1,1}^1$	150	0
22	M_2^2	$S_{1,1}^1$	150	0
23	$S_{1,2}^1$	D_1^2	200	12619
24	$S_{1,2}^1$	D_2^2	200	2565
25	$S_{1,2}^2$	D_1^1	32	0
26	$S_{1,2}^2$	D_2^1	32	0
27	0	1	525	0
28	0	2	525	0

6. Summary, Conclusions, and Suggestions for Future Research

The COVID-19 pandemic has vividly demonstrated the importance of and the need for tools from operations research and analytics. Faced with this global healthcare disaster, operations researchers have applied tools from simulation to game theory to enable deeper insights into all facets of gaining a greater understanding of the impacts and the management of this disaster as well as the response to it.

In this tutorial, game theory is overviewed, within the context of recently introduced new models inspired by the COVID-19 pandemic, along with the methodology of the theory of variational inequalities, which is applied for problem formulation, qualitative analysis, as well as computations. The theoretical foundations are recalled and three supply chain network based frameworks, drawn from the literature, with updates, presented. The first supply chain network game theory model overviewed in this tutorial is due to Nagurney (2021a). It incorporates labor as a critical resource and enables the investigation of the quantification of disruptions to labor, as well as changes to the productivity of labor. In the pandemic, the world has seen essential workers, who courageously serve as frontline workers, from the food industry to healthcare, getting ill from COVID-19, with the effects of labor shortages propagating in the associated supply chains and affecting not only local, but also global markets, and, of course, communities. This model is an example of a noncooperative game theory model, governed by a Nash equilibrium. The model provides the basis for other possible extensions, including those that have considered other types of constraints on labor (see, e.g., Nagurney (2021a, c)). Specifically, in the pandemic, we have seen workers in some sectors being retrained or reallocated to other sectors, where there was great need for labor. We have also seen migration of healthcare workers across many miles to provide much needed care and services in hospitals in regions severely impacted in different waves of the pandemic, and short of staff. It is expected that research on incorporating labor into the modeling of supply chains will continue, since truly, as noted in Nagurney (2021d), "in the end, it's all about people."

The second model is also a noncooperative game theory model, but governed by a Generalized Nash Equilibrium. It captures the intense competition for medical supplies in the COVID-19 pandemic, and also includes demand uncertainty. The model is of relevance to PPEs, ventilators, testing kits, and, now, even, COVID-19 vaccines. The reason that a Generalized Nash Equilibrium concept is needed for this application is that the supplies have been limited, and, therefore, the constraints faced by the various players in the game depend on one another's strategies and, of course, their respective utility functions do as well. The utility functions that the players seek to optimize are quite different from those in the first supply chain network application, which is focused on commercial supply chains. This work, due to Nagurney et al. (2021), has also recently stimulated the development of GNE models in which each player (which can even be a country) is faced with a two-stage stochastic optimization problem (see Salarpour and Nagurney (2021)). It is expected that the operations research based pandemic research will continue to make use of and, perhaps, also further integrate and extend the humanitarian operations and logistics literature.

The third model in this tutorial demonstrates how one can quantify the synergy associated with the possibility of cooperation among multiple organizations involved in multiple product supply chains involved in providing relief items in a disaster that can include a pandemic. The model also handles demand uncertainty, as well as cost uncertainty. The setup uses a mean variance approach. This work, due to Nagurney and Qiang (2020), can serve as the foundation for assessing possible public private partnerships and can even be integrated with labor constructs as in the first model in this tutorial. We expect that cooperation among relevant entities, including governments, will be essential in the continuing battles of this pandemic and in mitigating and preparing for future pandemics. Furthermore, it would be very worthwhile to investigate additional cooperative game theory concepts in the pandemic setting. For example, the use of the Bargaining Nash concept, which has been applied to the sharing of cybersecurity information (cf. Nagurney and Shukla (2017)), could be used to model partnerships even between competing pharmaceutical firms involved in vaccine production, to start.

It is also important to emphasize that rigorous supply chain network models, in both optimization and game theory settings, can be very useful for policymakers in the pandemic and beyond. For example, related optimization and game theory models, similar to those described in this tutorial have been constructed for blood supply chains by Nagurney, Masoumi, and Yu (2012), Masoumi, Yu, and Nagurney (2017), Dutta and Nagurney (2019), and Nagurney and Dutta (2019) and highlighted in the article by Nagurney (2020b). The latter article was referenced on the first page of the memo on the US blood supply by then California Attorney General Xavier Becerra to Admiral Brett Giroir, MD, then the Assistant Secretary for Health, U.S. Department of Health & Human Services, and signed by 21 other State Attorneys General (see Becerra (2020)) and helped to influence policy.

We expect that operations researchers' work will continue to be valued and recognized in the pandemic, harkening back to the discipline's origins and contributions in World War II. Indeed, it is times such as these, although very discomfiting and painful, that demonstrate what science can accomplish and the great impact of operations research, with its innovative models, efficient algorithms, and insights drawn from computational studies, on both decision-making and policy-making. The world, through the studies and writings, the presentations, and advocacy of members of our scientific discipline, now better understands and values supply chains, which are networks of connectivity for products that sustain life worldwide.

Acknowledgments

The author thanks INFORMS for the opportunity to prepare this tutorial. It is dedicated to all essential workers in the COVID-19 pandemic and beyond. The author acknowledges her collaborators and students, present and past, who make research so enjoyable. The author is grateful for the helpful comments and suggestions of two anonymous reviewers and the volume editor and TutORial chair, John Carlsson, on an earlier version of this tutorial. The author also acknowledges the INFORMS TutORials series editor, Douglas Shier, for additional assistance and comments. This TutORial is derived from a variety of previously published works by the author, as cited in this TutORial. She acknowledges the publishers, Elsevier (*European Journal of Operational Research*), Springer Nature (*Nonlinear Analysis and Global Optimization*), and IBM (*IBM Journal of Research and Development*), for publishing the articles from which Sections 3, 4, and 5, respectively, are derived.

References

Abraham, R., Maan, A., 2021. Global COVID-19 death toll surpasses 3 million amid new infections resurgence. Reuters.com, April 6. Available at:
https://www.reuters.com/article/us-health-coronavirus-global-casualties/global-covid-19-death-toll-surpasses-3-million-amid-new-infections-resurgence-idUSKBN2BT0V9

Associated Press, 2020. Coronavirus pandemic leads to Idaho potato market woes. April 27. Available at:
https://idahonews.com/news/coronavirus/coronavirus-pandemic-leads-to-idaho-potato-market-woes

Balcik, B., Beamon, B., 2008. Facility location in humanitarian relief. International Journal of Logistics: Research and Applications 11, 101-121.

Balcik, B., Beamon, B.M., Krejci, C.C., Muramatsu, K.M., Ramirez, M., 2010. Coordination in humanitarian relief chains: Practices, challenges and opportunities. International Journal of Production Economics 126(1), 22-34.

Barrero, J.M., Bloom, N., Davis, S. COVID-19 and labour reallocation: Evidence from the US. VoxEU.org, July 14. Available at:
https://voxeu.org/article/covid-19-and-labour-reallocation-evidence-us

Becerra, X., 20220. Re: Solicitation for Public Comments on Section 209 of the Pandemic and All-Hazards Preparedness and Advancing Innovation Act, 85 Fed. Reg. 16,372 (March 23, 2020). Available at:
https://www.washingtonblade.com/content/files/2020/04/States-Urge-FDA-to-Shift-Course.pdf

Bensoussan, A., 1974. Points de Nash dans le cas de fonctionelles quadratiques et jeux differentiels lineaires a N personnes. SIAM Journal on Control 12, 460-499.

Besik, D., Nagurney, A., 2017. Quality in competitive fresh produce supply chains with application to farmers' markets, Socio-Economic Planning Sciences 60, 62-76.

Bradsher, K., 2020. China dominates medical supplies, in this outbreak and the next. July 5, The New York Times. Available at: https://www.nytimes.com/2020/07/05/business/china-medical-supplies.html?smid= tw-nytimes&smtyp=cur

Burki, T., 2020. Global shortage of personal protective equipment. Lancet Infectious Diseases 20(7), 785-786.

Choi, T.-M., 2021. Fighting against COVID-19: What operations research can help and the sense-and-respond framework. Annals of Operations Research. In press: https://doi.org/10.1007/s10479-021-03973-w

Coles, J.B., Zhang, J., Zhuang, J., 2018. Partner selection in disaster relief: Partnership formation in the presence of incompatible agencies. International Journal of Disaster Risk Reduction 27, 94-108.

Coles, J.B., Zhuang, J., 2011. Decisions in disaster recovery operations: A game theoretic perspective on organization cooperation. Journal of Homeland Security and Emergency Management 8(1), Article 35.

Corbishley, N., 2020. Farm-labor crisis under COVID-19 sends countries scrambling. Wolf Street, April 13. Available at:
https://wolfstreet.com/2020/04/13/the-farm-labor-crisis-under-covid-19-and-how-countries-scramble-to-deal-with-it/

Corkery, M., Yaffe-Bellany, D., 2020. The food chain's weakest link: Slaughterhouses. The New York Times. April 18. Available at:
https://www.nytimes.com/2020/04/18/business/coronavirus-meat-slaughterhouses.html

Craighead, C.W., Ketchen Jr., D.J., Darby, J.L., 2020. Pandemics and supply chain management research: Toward a theoretical toolbox. Decision Sciences 51(4), 838-866.

Currie, C.S.M., Fowler, J.W., Kotiadis, K., Monks, T., Onggo, B.S., Robertson, D.A., 2020. How simulation modelling can help reduce the impact of COVID-19. Journal of Simulation 14(2), 83-97.

Dafermos, S., 1983. An iterative scheme for variational inequalities. Mathematical Programming 26, 40-47.

Debreu, G., 1952. A social equilibrium existence theorem. Proceedings of the National Academy of Sciences of the United States of America 38, 886-893.

Dong, J., Zhang, D., Nagurney, A., 2004. A supply chain network equilibrium model with random demands. European Journal of Operational Research 156, 194-212.

Dupuis, P., Nagurney, A., 1993. Dynamical systems and variational inequalities. Annals of Operations Research 44, 9-42.

Dutta, P., Nagurney, A., 2019. Multitiered blood supply chain network competition: Linking blood service organizations, hospitals, and payers. Operations Research for Health Care 23, 100230.

Facchinei, F., Kanzow, C., 2010. Generalized Nash equilibrium problems. Annals of Operations Research 175, 177-211.

Falasca, M., Zobel, C.W., 2011. A two-stage procurement model for humanitarian relief supply chains. Journal of Humanitarian Logistics and Supply Chain Management 1(2), 151-169.

Falcone, M., 2020. If nations compete for doses of coronavirus vaccines, we'll all lose. The Washington Post, December 9. Available at:https://www.washingtonpost.com/outlook/2020/12/09/if-nations-compete-doses-covid-19-vaccines-well-all-lose/

Fischer, A., Herrich, M., Schonefeld, K., 2014. Generalized Nash equilibrium problems - Recent advances and challenges. Pesquisa Operacional 34(3), 521-558.

Gabay, D., Moulin, H., 1980. On the uniqueness and stability of Nash equilibria in noncooperative games. In: Bensoussan, A., Kleindorfer, P., Tapiero, C.S. (Eds), Applied Stochastic Control of Econometrics and Management Science, North-Holland, Amsterdam, The Netherlands, pp 271-294.

Galinato, S., Gallardo, R., Hong, Y., 2016. 2015 cost estimates of establishing and producing conventional high bush blueberries in western Washington. Washington State University Extension, Pullman, Washington.

Gossler, T., Wakolbinger, T., Nagurney, A., Daniele, P., 2019. How to increase the impact of disaster relief: A study of transportation rates, framework agreements and product distribution. European Journal of Operational Research, 274(1), 126-141.

Grass, E., Fischer, K., 2016. Two-stage stochastic programming in disaster management: A literature survey. Surveys in Operations Research and Management Science 21(2), 85-100.

Haghani, A., Oh, S.C., 1996. Formulation and solution of a multi-commodity, multi-modal network flow model for disaster relief operations. Transportation Research A 30(3), 231-250.

Hardwick, A., 2020. Will the pandemic accelerate automation in supply chains? Part 1: Labour shortages in a time of high demand. Reuters, June 29. Available at:
https://www.eft.com/technology/will-pandemic-accelerate-automation-supply-chains-part-1-labour-shortages-time-high

Hartman, P., Stampacchia, G., 1966. On some nonlinear elliptic differential-functional equations. Acta Mathematica 115(1), 271-310.

Hopkins, J.S., 2021. To make more Covid-19 vaccines, rival drugmakers team up. The Wall Street Journal, February 23. Available at:
https://www.wsj.com/articles/to-make-more-covid-19-vaccines-rival-drugmakers-team-up-11614081601

howmuchisit.org, 2018. How much do blueberries cost? Available at:
https://www.howmuchisit.org/how-much-do-blueberries-cost/

Huang, M., Smilowitz, K., Balcik, B., 2012. Models for relief routing: Equity, efficiency and efficacy. Transportation Research E 48, 2-18.

IHS Markit, 2020. Coronavirus triggers acute farm labour shortages in Europe. August 4. Available at:
https://ihsmarkit.com/research-analysis/article-coronavirus-triggers-acute-farm-labour-shortages-europe.html

Ivanov, D., 2020. Predicting the impacts of epidemic outbreaks on global supply chains: A simulation-based analysis on the coronavirus outbreak (COVID-19/SARS-CoV-2) case. Transportation Research E 136, 101922.

Ivanov, D., Das, A., 2020. Coronavirus (COVID-19/SARS-CoV-2) and supply chain resilience: A research note. International Journal of Integrated Supply Management 13(1), 90-102.

Ivanov, D., Dolgui, A., 2020. Viability of intertwined supply networks: Extending the supply chain resilience angles towards survivability. A position paper motivated by COVID-19 outbreak. International Journal of Production Research 58(10), 2904-2915.

Kaplan, E.H., 2020. OM Forum - COVID-19 scratch models to support local decisions. Manufacturing & Service Operations Management 22(4), 645-655.

Karamardian, S., 1969. The nonlinear complementarity problem with applications, Part 1. Journal of Optimization Theory and Applications 4, 87-98.

Kinderlehrer, D., Stampacchia, G., 1980. An Introduction to Variational Inequalities and Their Applications. Academic Press, New York.

Knight, V., 2020. Without federal protections, farm workers risk coronavirus infection to harvest crops. NPR, August 8. Available at:
https://www.npr.org/sections/health-shots/2020/08/08/900220260/without-federal-protections-farm-workers-risk-coronavirus-infection-to-harvest-c

Korpelevich, G.M., 1977. The extragradient method for finding saddle points and other problems. Matekon 13, 35-49.

Kotsireas, I.S., Nagurney, A., Pardalos, P.M., Editors, 2018. Dynamics of Disasters: Algorithmic Approaches and Applications. Springer International Publishing Switzerland.

Kotsireas, I.S., Nagurney, A., Pardalos, P.M., Tsokas, A., Editors, 2021. Dynamics of Disasters - Impact, Risk, Resilience, and Solutions, Springer Nature Switzerland AG.

Kulkarni, A.A., Shanbhag, U.V., 2012. On the variational equilibrium as a refinement of the generalized Nash equilibrium. Automatica 48, 45-55.

Mamani, H., Chick, S.E., Simchi-Levi, D., 2013. A game-theoretic model of international influenza vaccination coordination. Management Science 59(7), 1650-1670.

Masoumi, A.H., Yu, M., Nagurney, A., 2017. Mergers and acquisitions in blood banking systems: A supply chain network approach. International Journal of Production Economics 193, 406-421.

Mete, H.O., Zabinsky, Z.B., 2010. Stochastic optimization of medical supply location and distribution in disaster management. International Journal of Production Economics 126(1), 76-84.

Mishra, S.K., 2007. A brief history of production functions. MPRA Paper No. 5254, http://mpra.ub.uni-muenchen.de/5254/.

Muggy L., Heier Stamm, J.L., 2014. Game theory applications in humanitarian operations: A review. Journal of Humanitarian Logistics and Supply Chain Management 4(1), 4-23.

Nagurney, A., 1999. Network Economics: A Variational Inequality Approach, second and revised edition. Boston, Massachusetts: Kluwer Academic Publishers.

Nagurney, A., 2006. Supply Chain Network Economics: Dynamics of Prices, Flows, and Profits. Edward Elgar Publishing, Cheltenham, United Kingdom.

Nagurney, A., 2009. A system-optimization perspective for supply chain integration: The horizontal merger case. Transportation Research E 45, 1-15.

Nagurney, A., 2020a. The raging competition for medical supplies is not a game, but game theory can help. The Conversation, August 4. Available at:
https://theconversation.com/the-raging-competition-for-medical-supplies-is-not-a-game-but-game-theory-can-help-143514

Nagurney, A., 2020b. How coronavirus is upsetting the blood supply chain. The Conversation, March 12. Available at:

https://theconversation.com/how-coronavirus-is-upsetting-the-blood-supply-chain-133424

Nagurney, A., 2021a. Supply chain game theory network modeling under labor constraints: Applications to the COVID-19 pandemic. European Journal of Operational Research 293(3), 880-891.

Nagurney, A., 2021b. Perishable food supply chain networks with labor in the Covid-19 pandemic. In: Dynamics of Disasters - Impact, Risk, Resilience, and Solutions, I.S. Kotsireas, A. Nagurney, P.M. Pardalos, and A. Tsokas, Editors, Springer International Publishing Switzerland, pp 173-193.

Nagurney, A., 2021c. Optimization of supply chain networks with inclusion of labor: Applications to COVID-19 pandemic disruptions. International Journal of Production Economics 235, 108080.

Nagurney, A., 2021d. In the end, it's all about people. ORMS Today, January 29. Available at: https://pubsonline.informs.org/do/10.1287/orms.2021.01.17/full/#.YHwTE1wXjAI.twitter

Nagurney, A., Alvarez Flores, E., Soylu, C., 2016. A Generalized Nash Equilibrium model for post-disaster humanitarian relief. Transportation Research E 95, 1-18.

Nagurney, A., Daniele, P., Alvarez Flores, E., Caruso, V., 2018. A variational equilibrium network framework for humanitarian organizations in disaster relief: Effective product delivery under competition for financial funds. In: Dynamics of Disasters: Algorithmic Approaches and Applications, I.S. Kotsireas, A. Nagurney, and P.M. Pardalos, Editors, Springer International Publishing Switzerland, pp 109-133.

Nagurney, A., Daniele, P., Cappello, G., 2021. Capacitated human migration networks and subsidization. In: Dynamics of Disasters - Impact, Risk, Resilience, and Solutions, I.S. Kotsireas, A. Nagurney, P.M. Pardalos, and A. Tsokas, Editors, Springer International Publishing Switzerland, pp 195-217.

Nagurney, A., Dutta, P., 2019. Competition for blood donations. Omega 212, 103-114.

Nagurney, A., Masoumi, A.H., 2012. Supply chain network design of a sustainable blood banking system. In: Sustainable Supply Chains: Models, Methods and Public Policy Implications, T. Boone, V. Jayaraman, and R. Ganeshan, Editors, Springer, London, England, pp 49-72.

Nagurney, A., Masoumi, A., Yu, M., 2012. Supply chain network operations management of a blood banking system with cost and risk minimization. Computational Management Science 9(2), 205-231.

Nagurney, A., Masoumi, A.H., Yu, M., 2015. An integrated disaster relief supply chain network model with time targets and demand uncertainty. In: Regional Science Matters: Studies Dedicated to Walter Isard, P. Nijkamp, A. Rose, and K. Kourtit, Editors, Springer International Publishing

Switzerland, pp 287-318.

Masoumi, A.H., Yu, M., Nagurney, A., 2017. Mergers and acquisitions in blood banking systems: A supply chain network approach. International Journal of Production Economics 193, 406-421.

Nagurney, A., Nagurney, L.S., 2016. A mean-variance disaster relief supply chain network model for risk reduction with stochastic link costs, time targets, and demand uncertainty. In: Dynamics of Disasters: Key Concepts, Models, Algorithms, and Insights, I. Kotsireas, A. Nagurney, and P.M. Pardalos, Editors, Springer International Publishing Switzerland, pp 231-255.

Nagurney, A., Qiang, Q., 2009. Fragile Networks: Identifying Vulnerabilities and Synergies in an Uncertain World. John Wiley & Sons, Hoboken, New Jersey.

Nagurney, A., Qiang, A., 2020. Quantifying supply chain network synergy for humanitarian organizations. IBM Journal of Research and Development 64(1/2), 12:1-12:16.

Nagurney, A., Salarpour, M., Daniele, P., 2019. An integrated financial and logistical game theory model for humanitarian organizations with purchasing costs, multiple freight service providers, and budget, capacity, and demand constraints. International Journal of Production Economics 212, 212-226.

Nagurney, A., Salarpour, M., Dong, J., Dutta, P., 2021. Competition for medial supplies under stochastic demand in the COVID-19 pandemic: A Generalized Nash Equilibrium framework. In: Nonlinear Analysis and Global Optimization, T.M. Rassias and P.M. Pardalos, Editors, Springer Nature Switzerland AG, pp 331-356.

Nagurney, A., Salarpour, M., Dong, J., Nagurney, L.S., 2020. A stochastic disaster relief game theory network model. Operations Research Forum 1, 10.

Nagurney, A., Shukla, S., 2017. Multifirm models of cybersecurity investment competition vs. cooperation and network vulnerability. European Journal of Operational Research 260(2), 588-600.

Nagurney, A., Woolley, T., Qiang, Q., 2010. Multiproduct supply chain horizontal network integration: Models, theory, and computational results. International Transactions in Operational Research 17, 333-349.

Nagurney, A., Yu, M., Besik, D., 2017. Supply chain network capacity competition with outsourcing: A variational equilibrium framework. Journal of Global Optimization 69 (1), 231-254.

Nagurney, A., Yu, M., Masoumi, A.H., Nagurney, L.S., 2013. Networks Against Time: Supply Chain Analytics for Perishable Products. Networks Against Time: Supply Chain Analytics for

Perishable Products. Springer Science+Business Media, New York, NY.

Nagurney, A., Yu, M., Qiang, Q., 2011. Supply chain network design for critical needs with outsourcing. Papers in Regional Science 90, 123-142.

Nagurney, A., Zhang, D., 1996. Projected Dynamical Systems and Variational Inequalities with Applications. Kluwer Academic Publishers, Boston, Massachusetts.

Nash, J.F., 1950. Equilibrium points in n-person games. Proceedings of the National Academy of Sciences, USA 36, 48-49.

Nash, J.F., 1951. Noncooperative games. Annals of Mathematics 54, 286-298.

O'Connell, J., 2020. Doctors say their PPE supply could run dry in weeks. The TimesTribune, July 6. Available at:
https://www.thetimes-tribune.com/news/coronavirus/doctors-say-their-ppe-supply-could-run-dry-in-weeks/article_5a0751c7-a153-598e-99fa-a8cab61d71e4.html

Ozdamar, L., Ekinci, E., Kkyazici, B., 2004. Emergency logistics planning in natural disasters. Annals of Operations Research 129(1-4), 217-245.

Paul, S.K., Chowdhury, P., 2020. A production recovery plan in manufacturing supply chains for a high-demand item during COVID-19. In press in: International Journal of Physical Distribution & Logistics Management. doi: 10.1108/IJPDLM-04-2020-0127

Polansek, T., Huffstutter, P.J., 2020. Piglets aborted, chickens gassed as pandemic slams meat sector. Reuters, April 27. Available at: https://www.reuters.com/article/us-health-coronavirus-livestock-insight/piglets-aborted-chickensgassed-as-pandemic-slams-meat-sector-idUSKCN2292YS

Queiroz, M.M., Ivanov, D., Dolgui, A., Wamba, S.F., 2020. Impacts of epidemic outbreaks on supply chains: Mapping a research agenda amid the COVID-19 pandemic through a structured literature review. Annals of Operations Research, 1-38.

Raker, E.J., Zacher, M., Lowe, S.R., 2020. Lessons from Hurricane Katrina for predicting the indirect health consequences of the COVID-19 pandemic. Proceedings of the National Academy of Sciences, 117(23), 12595-12597.

Ranney, M.L., Griffeth, V., Jha, A.K., 2020. Critical supply shortages – The need for ventilators and Personal Protective Equipment during the Covid-19 pandemic. The New England Journal of Medicine. April 30.DOI: 10.1056/NEJMp2006141

Rawls, C.G., Turnquist, M.A., 2010. Pre-positioning of emergency supplies for disaster response.

Transportation Research B 44(4), 521-534.

Revill, J., Farge, E., 2021. Real COVID-19 death toll could be ‘two to three’ times above official stats: WHO. Reuters, May 21. Available at:
https://www.reuters.com/world/covid-19-death-tolls-are-likely-significant-undercount-who-says-2021-05-21/

Rosen, J.B., 1965. Existence and uniqueness of equilibrium points for concave N-person games. Econometrica 33, 520-534.

Russell, E., 2020. COVID-19 cases among blueberry workers worsen farm labor shortage. Portland Press Herald, Portland, Maine. Available at:
https://www.pressherald.com/2020/08/03/covid-19-cases-among-blueberry-workers-worsen-farm-labor-shortage/

Salarpour, M., Nagurney, A., 2021. A multicountry, multicommodity stochastic game theory network model of competition for medical supplies inspired by the Covid-19 pandemic. International Journal of Production Economics 236, 108074.

Salmeron, J., Apte, A., 2010. Stochastic optimization for natural disaster asset prepositioning. Production and Operations Management 19(5), 561-574.

Seaberg, D., Devine, L., Zhuang, J., 2017. A review of game theory applications in natural disaster management research. Natural Hazards 89, 1461-1483.

Shea, A., 2020. From dirt to doorstep, during coronavirus crisis Massachusetts farms find ways to come to you. WBUR, March 31. Available at:
https://www.wbur.org/artery/2020/03/31/with-markets-closed-farmers-bring-fresh-food-to-their-customers-doorstep

Stemple, K., 2019. Migration surge from Central America was spurred, in part, by Mexican policies. The New York Times, April 1. Available at:
https://www.nytimes.com/2019/04/01/world/americas/mexico-migration-border.html

Toyasaki, F., Arikan, E., Silbermayr, L., Falagara Sigala, I., 2017. Disaster relief inventory management: Horizontal cooperation between humanitarian organizations. Production and Operations Management 26(6), 1221-1237.

Toyasaki, F., Wakolbinger, T., 2014. Impacts of earmarked private donations for disaster fundraising. Annals of Operations Research 221, 427-447.

Tully, T., 2020. How you get your berries: Migrant workers who fear virus, but toil on. The New

York Times, July 5.

Tzeng, G.-H., Cheng, H.-J., Huang, T., 2007. Multi-objective optimal planning for designing relief delivery systems. Transportation Research E 43(6), 673-686.

van Hoek, 2020. Research opportunities for a more resilient post-COVID-19 supply chain - closing the gap between research findings and industry practice. International Journal of Operations & Production Management 40(4), 341-355.

Van Wassenhove, L.N,. 2006. Humanitarian aid logistics: Supply chain management in high gear. Journal of the Operational Research Society 57(5), 475-489.

Vitoriano, B., Ortuno, M., Tirado, G., Montero, M., 2011. A multi-criteria optimization model for humanitarian aid distribution. Journal of Global Optimization 51, 189-208.

Walsh, J., 2021. Competition among Minnesotans for vaccine shots heats up. Star Tribune. March 26. Available at:
https://www.startribune.com/competition-among-minnesotans-for-vaccine-shots-heats-up/600039219/

Wan, W., 2020. America is running short on masks, gowns and gloves. Again. The Washington Post, July 8. Available at:
https://www.washingtonpost.com/health/2020/07/08/ppe-shortage-masks-gloves-gowns/

Whalen, J., Albergotti, R., Lynch, D.J., 2021. Biden can't fix the chip shortage any time soon. Here's why. The Washington Post, March 1. Available at:
https://www.washingtonpost.com/technology/2021/03/01/semiconductor-shortage-halts-auto-factories/

Woolever, L., 2020. Local farms embrace change in the face of coronavirus. Baltimore Magazine, April 6. Available at:
https://www.baltimoremagazine.com/section/fooddrink/local-farms-embrace-change-in-the-face-of-coronavirus

World Health Organization, 2020. WHO Director-General's opening remarks at the media briefing on COVID-19 - 11 March 2020. Genevva, Switzerland. Available at:
https://www.who.int/dg/speeches/detail/who-director-general-s-opening-remarks-at-the-media-briefing-on-covid-19—11-march-2020

Yi, W., Kumar, A., 2007. Ant colony optimization for disaster relief operations. Transportation Research E 43(6), 660-672.

Yi, W., Ozdamar, L., 2007. A dynamic logistics coordination model for evacuation and support in disaster response activities. European Journal of Operational Research 179(3), 1177-1193.

Yu, M., Nagurney, A., 2013. Competitive food supply chain networks with application to fresh produce. European Journal of Operational Research 224(2), 273-282.